rbfox1 LoF mutants show disrupted *bdnf/trkb2* and *crhb/nr3c2* expression and increased cortisol levels during development coupled with signs of allostatic overload in adulthood

Adele Leggieri[1], Judit García-González[2], Saeedeh Hosseinian[1], Peter Ashdown[1], Sofia Anagianni[1], Xian Wang[1], William Havelange[1], Noèlia Fernàndez-Castillo[3,4,5,6], Bru Cormand[3,4,5,6] and Caroline H. Brennan[1]*

1 Centre for Brain and Behaviour, School of Biological and Behavioural Sciences, Queen Mary University of London, Mile End Rd, London, E1 4NS, United Kingdom

2 Department of Genetics and Genomic Sciences, Icahn School of Medicine, Mount Sinai, New York City, NY 10029, USA

3 Departament de Genètica, Microbiologia i Estadística, Facultat de Biologia, Universitat de Barcelona, Barcelona, Catalunya, 08028, Spain

4 Centro de Investigación Biomédica en Red de Enfermedades raras (CIBERER), Spain

5 Institut de Biomedicina de la Universitat de Barcelona, Barcelona, Catalunya, 08028, Spain

6 Institut de recerca Sant Joan de Déu, Espluges de Llobregat, Catalunya, 08950, Spain

*** Correspondence:** Caroline H. Brennan, c.h.brennan@qmul.ac.uk

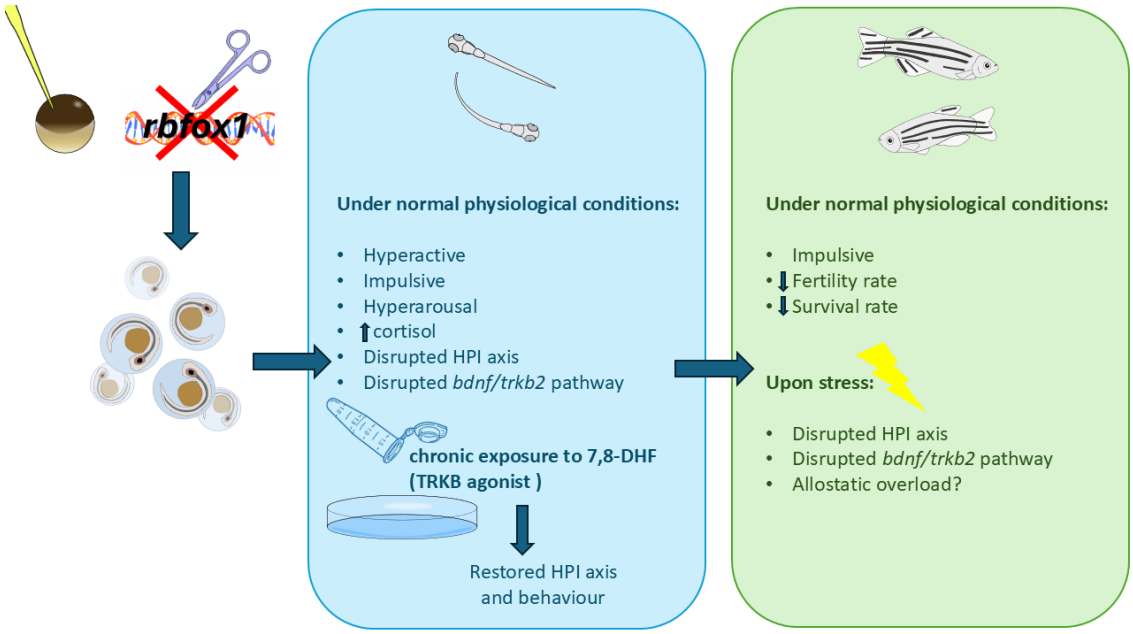

ABSTRACT

Mutations in the *RBFOX1* gene are associated with psychiatric disorders but how RBFOX1 influences psychiatric disorder vulnerability remains unclear. Recent studies showed that RBFOX proteins mediate the alternative splicing of PAC1, a critical HPA axis activator. Further, RBFOX1 dysfunction is linked to dysregulation of BDNF/TRKB, a pathway promoting neuroplasticity, neuronal survival, and stress resilience. Hence, RBFOX1 dysfunction may increase psychiatric disorder vulnerability via HPA axis dysregulation, leading to disrupted development and allostatic overload. To test this hypothesis, we generated a zebrafish *rbfox1* loss of function (LoF) line and examined behavioural and molecular effects during development. We found that *rbfox1* LoF mutants exhibited hyperactivity, impulsivity and heightened arousal, alongside alterations in proliferation – traits associated with neurodevelopmental and stress-related disorders. In adults, loss of *rbfox1* function led to decreased fertility and survival, consistent with allostatic overload. At the molecular level, at larval stages *rbfox1* mutants showed increased cortisol levels and disrupted expression of key stress-related genes (*bdnf, trkb2, pac1a-hop, crhb, nr3c2*). Pharmacological intervention targeting TRKB restored *crhb* and *nr3c2* gene expression and hyperactive and hyperarousal behaviours. In adults, dysregulation of *crhb, nr3c2* and *bdnf/trkb2* genes was only seen following acute stress exposure. Our findings reveal a fundamental role for RBFOX1 in integrating stress responses through its regulation of BDNF/TRKB and neuroendocrine signalling.

INTRODUCTION

Psychiatric disorders are influenced by multiple genes, with a substantial portion of their heritability linked to common genetic variations[1]. Identifying gene variants associated with multiple psychiatric disorders is crucial for understanding their shared genetic underpinnings and enhancing therapeutic strategies.

RNA binding fox-1 homologue 1 (RBFOX1), also known as FOX1 or ataxin 2-binding protein 1 (A2BP1), is a splicing factor highly conserved among vertebrates and expressed in the heart, brain and skeletal muscle, where it contributes to normal development and function[2,3]. Alterations in *RBFOX1* expression or function have been associated with susceptibility to psychiatric disorders, particularly those associated with changes in stress-related behaviour[4–6]. In a cross-disorder genome-wide association study (GWAS), *RBFOX1* emerged as the second most pleiotropic *locus*, showing association with seven out of the eight disorders studied: schizophrenia, bipolar disorder, depression, attention-deficit/hyperactivity disorder (ADHD), autism spectrum disorder (ASD), obsessive-compulsive disorder and Tourette syndrome[1]. In mice and zebrafish, *Rbfox1/rbfox1* knockout caused hyperactivity, increased anxiety-like behaviour and altered social behaviour[2,6]. However, the mechanisms by which *RBFOX1* genetic variants contribute to psychiatric disease are poorly understood.

In both mice and zebrafish, it has been suggested that Rbfox1 regulates the Pituitary Adenylate Cyclase-Activating Polypeptide Type 1 Receptor (Pac1) alternative splicing, an important mediator of corticotropin releasing hormone (CRH) synthesis in the hypothalamus[4,7]. CRH is the first hormone to be secreted in response to stress by the hypothalamic-pituitary-adrenal (HPA) axis (hypothalamic-pituitary-interrenal (HPI) axis in fish)[8]. In mammals there are several PAC1 isoforms with the predominant isoforms in the brain being PAC1-hop (long isoform) and PAC1-short[9]. In mice and zebrafish, following acute stress exposure, both *Pac1-hop/pac1-hop* and *Pac1-short/pac1-short* expression increased, while at the late recovery phase, only *Pac1-hop* was still up-regulated[4].

Another regulator of the stress response and a resilience factor against chronic stress-induced psychopathology is the brain derived neurotrophic factor (BDNF)/Tropomyosin receptor kinase B (TRKB) pathway[10–12]. BDNF is a neurotrophin possessing a pivotal role in the modulation of neurotransmission and synaptic plasticity and dysregulation of the BDNF/TRKB pathway has been associated with several neuropsychiatric diseases, including anxiety/stress disorders[13,14]. In human neural stem cells, *RBFOX1* knockdown increased *BDNF* expression levels[15], while another study in mice identified *TrkB* as a target of RBFOX1 within the hippocampus[16]. Further, PAC1-short activation can elevate *BDNF* levels and potentiate TRKB activity, enhancing BDNF/TRKB neuroprotective and plasticity-promoting effects, especially in the context of stress response and neuropsychiatric health[17].

Given that both PAC1 and BDNF/TRKB influence how the brain adapts to and manages stress, RBFOX1 variants may increase susceptibility to psychiatric disorders through dysregulation of the stress response, leading to adaptive plasticity and disrupted development in the short-term and allostatic overload in the long-term. Allostasis refers to the collective processes by which the body actively maintains stability (or homeostasis) in response to environmental stressors[12]. When allostasis primary mediators (e.g., HPA axis hormones, catecholamines, cytokines) are overactivated or fail to return to normal, it leads to an allostatic state[18,19]. The cumulative results of an allostatic state are referred to as allostatic load and, when maladaptive, allostatic overload[18]. Excess glucocorticoid exposure during early life and early life stress have been shown to cause prolonged activation of the allostatic systems, ultimately leading to allostatic overload[19–22], while neurotrophic factors such as BDNF play a key role in regulating adaptive plasticity and mechanisms counteracting damage caused by allostatic overload[12]. Here, to explore the possibility that *RBFOX1* loss of function (LoF) leads to increased vulnerability to psychiatric disease through HPA axis hyperactivation and allostasis-induced adaptation during development, we generated a zebrafish line carrying a predicted *rbfox1* LoF mutation using CRISPR-Cas9 gene editing and assessed behavioural and molecular changes at different developmental stages. We hypothesized that RBFOX1 regulates HPA axis activity through an effect on BDNF/TRKB signalling leading to disrupted brain development.

RESULTS

Generation of a loss of function *rbfox1* line

CRISPR-Cas9 genome editing generated a 19 base pair deletion (NM_001005596.1, nucleotides 120-138, TCCCATCGGCCCAGTTCGC) that introduced a premature termination codon (PTC) at position 58 in the *rbfox1* amino acid sequence. This line is recorded on ZFIN as qm4, ZDB-ALT-240222-6. Details regarding the generation of the line, nucleotide and amino acid sequences can be found in our previous study[2]. Wild type animals are denoted throughout as $rbfox1^{+/+}$, heterozygous mutants as $rbfox1^{+/19del}$ and homozygous mutants as $rbfox1^{19del/19del}$.

To evaluate whether the PTC elicited mRNA non-sense mediated decay (NMD) and consequent reduction of *rbfox1* mRNA in mutant fish, we examined *rbfox1* expression by quantitative Real-Time polymerase chain reaction (qPCR) and by *in situ* hybridisation (ISH). As *RBFOX1* itself is alternatively spliced to generate nuclear and cytoplasmic isoforms[7], we designed primers targeting all *rbfox1* zebrafish isoforms available on NCBI (see Supplementary Table1). qPCR showed that *rbfox1* transcript levels were significantly lower in mutant larvae compared to $rbfox1^{+/+}$ siblings ($p_{rbfox1^{+/+}\ vs\ rbfox1^{+/19del}} < 0.05$, $p_{rbfox1^{+/+}\ vs\ rbfox1^{19del/19del}} < 0.01$), and ISH showed that *rbfox1* was not detectable in $rbfox1^{19del/19del}$ fish, at either larval or adult stages (Supplementary Figure 1A-C).

These results confirm degradation of defective *rbfox1* mRNA in mutant fish.

112

113 ***rbfox1* mutant fish show hyperactivity, impulsivity and hyperarousal behaviour**

114 As mutations in *RBFOX1* locus have been linked to several psychiatric diseases in humans, we
115 assessed zebrafish larvae and adult fish for phenotypic traits associated with such disorders and
116 examined *rbfox1* mRNA distribution in *rbfox1*$^{+/+}$ larvae and adults (Tübingen strain).
117
118 In humans, *RBFOX1* copy number variants (CNVs) and LoF mutations are risk factors for ADHD[6]. Two
119 major ADHD traits are hyperactivity and increased impulsivity. We therefore assessed hyperactive
120 and impulsive behaviour of *rbfox1*$^{+/+}$, *rbfox1*$^{+/19del}$ and *rbfox1*$^{19del/19del}$ 5 days post fertilization (dpf)
121 larvae and adults. When we measured larval locomotion, we observed a gene dosage effect on
122 distance travelled, whereby *rbfox1* mutant larvae travelled greater distances than wild type siblings
123 ($p_{rbfox1^{+/+} \text{ vs } rbfox1^{+/19del}} < 0.05$, $p_{rbfox1^{+/+} \text{ vs } rbfox1^{19del/19del}} < 0.0001$, $p_{rbfox1^{+/19del} \text{ vs } rbfox1^{19del/19del}} < 0.05$)
124 (Supplementary Figure 2A), and a significant increase in the swimming speed of *rbfox1*$^{19del/19del}$ larvae
125 ($p_{rbfox1^{+/+} \text{ vs } rbfox1^{19del/19del}} < 0.0001$, $p_{rbfox1^{+/19del} \text{ vs } rbfox1^{19del/19del}} < 0.05$) (Supplementary Figure 2B). This is
126 in line with hyperactivity observed in adult *rbfox1*$^{19del/19del}$, in our previous study and in other *rbfox1*
127 model[2,23]. We also measured larval burst swimming, a parameter previously used as a measure to
128 predict impulsive behaviour in zebrafish larvae[24]. We found a significant increase in the number of
129 peaks (acceleration events when the fish travelled > 5 mm in < 12 sec) in *rbfox1*$^{19del/19del}$ larvae (p
130 $_{rbfox1^{+/+} \text{ vs } rbfox1^{19del/19del}} < 0.0001$, $p_{rbfox1^{+/19del} \text{ vs } rbfox1^{19del/19del}} < 0.0001$) (Figure 1A). Impulsive behaviour
131 was then assessed in adult (7 months old) fish using the 5-choice serial reaction time task (5-
132 CSRTT)[25]. The 5-CSRTT assay measures sustained attention and impulsive action by requiring an
133 animal to detect a brief visual cue (white light stimulus) presented randomly across one of five
134 apertures and "nosepoke" that aperture to signal recognition (Supplementary Figure 3). If correct, a
135 "food" signal light comes on (at the opposite end of the test chamber) and the animal collects food
136 reward (Supplementary Figure 3). Crucially, a pause occurs prior to the onset of the stimulus light
137 (called a pre-stimulus interval [PSI]), during which a 'premature' response can be interpreted as
138 'impulsivity'- impulsive action[25]. The assay consists of five stages (Supplementary Table2) each run
139 for at least a week until fish are promoted to the next stage. We found that 79% *rbfox1*$^{+/+}$, 72%
140 *rbfox1*$^{+/19del}$ and 62% *rbfox1*$^{19del/19del}$ learned the task within 9 weeks. We found no significant
141 differences in the correct responses (stages 2-5, Figure 1B-E). In stage 5, we found a significant
142 difference in the number of premature responses (increased impulsivity) such that *rbfox1*$^{19del/19del}$
143 fish were more impulsive compared to *rbfox1*$^{+/+}$ siblings ($p < 0.05$) (Figure 1F).

144 *RBFOX1* CNVs have also been identified in individuals with schizophrenia[6,15]. Deficits in habituation
145 to acoustic startle reflex are seen in both schizophrenic patients and animal models of
146 schizophrenia[26]. The acoustic startle assay has been widely employed to measure habituation in
147 animals, including zebrafish[27]. The magnitude of the startle response and the extent of habituation
148 can also serve as indicators of hyperarousal linked to heightened stress responses[28]. We therefore
149 tested 5dpf zebrafish larvae (*rbfox1*$^{+/+}$, *rbfox1*$^{+/19del}$ and *rbfox1*$^{19del/19del}$) in the habituation to acoustic
150 startle response assay. Consistent with our hyperactivity assay, during the baseline (first 10 min), the
151 genotype had a significant main effect on distance travelled [Effect of genotype: $\chi2(2) = 8.3397$, $p <$
152 0.05] whereby *rbfox1*$^{19del/19del}$ larvae travelled greater distances than *rbfox1*$^{+/+}$ siblings ($p < 0.05$).
153 During the startle stimuli, we observed a main effect of genotype [Effect of genotype: $\chi2(2) = 33.536$,
154 $p < 0.0001$] and stimulus number [Effect of stimulus number: $\chi2(9) = 487.968$, $p < 0.0001$] on
155 distance travelled, and a significant two-way interaction between genotype and stimulus number
156 [Effect of genotype by stimuli: $\chi2(18) = 31.511$, $p < 0.05$], whereby *rbfox1*$^{19del/19del}$ larvae travelled
157 greater distances than *rbfox1*$^{+/+}$ ($p < 0.001$) and *rbfox1*$^{+/19del}$ ($p < 0.01$) (Supplementary Figure 2C).
158 When assessed for the rate of habituation, wild type larvae showed a habituation response to
159 repeated acoustic startle consistent with previous reports[29]: 100% of *rbfox1*$^{+/+}$animals responded to
160 the first acoustic stimulus, but only 22% responded to the last. When we examined the rate of

habituation over time, in line with previous findings[30], we observed a significant genotype effect [Effect of genotype: $\chi2(2) = 7.2676$, $p < 0.05$] and a significant two-way interaction between genotype and stimulus number [Effect of genotype by stimulus number: $\chi2(18) = 132.8476$, $p < 0.001$] whereby *rbfox1*$^{19del/19del}$ showed reduced rate of habituation and a greater proportion of responders compared to *rbfox1*$^{+/+}$ siblings ($p_{rbfox1^{+/+} \text{ vs } rbfox1^{19del/19del}} < 0.05$) (Supplementary Figure 2D).

SNPs in *RBFOX1* locus have also been associated with anxiety[6,31]. Hence, we assessed anxiety-like behavior in 5dpf zebrafish larvae using the forced light-dark transition (FLDT) assay and in adult zebrafish using the novel tank diving (NTD) assay. In the FLDT assay, zebrafish are exposed to sudden transitions in illumination with effects on locomotion and amplitude of response on transition from dark to light being used as a measure of anxiety-like behaviour: the increased locomotion/startle response upon the light-dark transition is a measure of anxiety-like behaviour[29,32,33]. Consistent with our acoustic startle assay, we found that during the baseline (first 5 min) (Figure 1G) genotype had a significant main effect on distance travelled [Effect of genotype: $\chi2(2) = 14.4878$, $p < 0.001$] whereby *rbfox1*^{19del} larvae travelled greater distances than *rbfox1*$^{+/+}$ siblings ($p_{rbfox1^{+/+} \text{ vs } rbfox1^{+/19del}} < 0.05$, $p_{rbfox1^{+/+} \text{ vs } rbfox1^{19del/19del}} < 0.01$). During the 1min light flash (min 5-6 of the assay) we found a significant main effect of genotype on distance travelled [Effect of genotype: $\chi2(2) = 8.8518$, $p < 0.05$] with *rbfox1*^{19del} larvae travelling greater distances than *rbfox1*$^{+/+}$ siblings ($p_{rbfox1^{+/+} \text{ vs } rbfox1^{+/19del}} < 0.05$, $p_{rbfox1^{+/+} \text{ vs } rbfox1^{19del/19del}} < 0.05$) (Figure 1H). On transition from dark to light (analysed at 1 sec time bin resolution from sec 240 to sec 360 as the startle response during the transition is visible only at this resolution) we found a significant main effect of time [Effect of time: $\chi2(118) = 1051.3482$, $p < 0.001$] and genotype [Effect of genotype: $\chi2(2) = 8.9155$, $p < 0.05$], and a significant two-way interaction between time and genotype [Effect of time by genotype: $\chi2(236) = 514.8308$, $p < 0.001$] on the amplitude of response, whereby *rbfox1*$^{19del/19del}$ larvae startled more than *rbfox1*$^{+/+}$ ($p < 0.05$) and *rbfox1*$^{+/19del}$ ($p < 0.05$) siblings (Figure 1H). As there was a significant difference in basal locomotion, we also examined the amplitude of response on transition from dark to light normalizing the data against baseline, as reported previously[34]. We observed similar results as in absence of normalisation: significant main effect of time [Effect of time: $\chi2(118) = 1249.918$, $p < 0.001$] and genotype [Effect of genotype: $\chi2(2) = 37.716$, $p < 0.001$], and a significant two-way interaction between time and genotype [Effect of time by genotype: $\chi2(236) = 4532.966$, $p < 0.001$] whereby *rbfox1*$^{19del/19del}$ larvae startled more than *rbfox1*$^{+/+}$ ($p < 0.0001$) and *rbfox1*$^{+/19del}$ ($p < 0.001$) siblings.

Anxiety-like behaviour in adult animals was assessed using the NTD assay. When introduced to a novel tank, zebrafish will first dive to the bottom of the tank, to seek protection, and then gradually increase their swimming over time[35]. Over the entire duration of the NTD assay, we found no significant differences between *rbfox1* genotypes($p > 0.05$). However, during the first minute of the assay, we found a significant two-way interaction between genotype and the time spent at the bottom of the tank [Effect of genotype by proportion at the bottom tank: $\chi2(10) = 22.3333$, $p < 0.05$], such that *rbfox1*$^{19del/19del}$ fish spent less time in the bottom than *rbfox1*$^{+/+}$ fish ($p < 0.001$) (Supplementary Figure 2E). In line with previous findings[2], we observed no significant differences in distance travelled ($p > 0.05$) (Supplementary Figure 3F), nor in the number of the transitions to the top area of the tank between *rbfox1* genotypes ($p > 0.05$) (Supplementary Figure 3E).

Thus, our data showed that loss of *rbfox1* resulted in behavioural changes in zebrafish that are relevant to core domains often altered in human psychiatric disorders (such as hyperactivity, impulsivity, reduced habituation and heightened arousal) and suggest that adaptation occurs as the animal develops.

209

210 ***rbfox1* is expressed in the developing neural and cardiac tissues and in adult brain regions involved**
211 **in stress, social and emotional behaviours, reward and learning**
212

213 Consistent with our behavioural results and as seen previously[2,3], when we assessed *rbfox1* mRNA
214 distribution in *rbfox1*$^{+/+}$ larvae and adults (Tübingen strain), we found that *rbfox1* was expressed in
215 regions of the brain involved in the response to stress, in social and emotional behaviour, and in
216 reward and learning (Figure 1A-B) in agreement with data in rodents[36] and humans[37].

217 In wild type larvae *rbfox1* is expressed in the spinal cord and hindbrain lateral neurons (Figure 1A, 28
218 hpf), whereas at later developmental stages, *rbfox1* expression was detected in the mid- and
219 hindbrain (Figure 1A, 2-5 dpf) and in the heart (Figure 1A, 5dpf) as described previously[38].

220 In adult fish, *rbfox1* is expressed along the entire whole rostro-caudal brain axis. In the forebrain,
221 *rbfox1* was detected in the glomerular (GL), internal (ICL), external (ECL) cellular layers of the
222 olfactory bulbs (Figure 1B a, a'). More caudally, *rbfox1* expression was detected in the medial zone of
223 the dorsal telencephalic area (Dm), and in the dorsal (Vd), lateral (Vl) and ventral (Vv) nuclei of the
224 ventral telencephalic area (Figure 1B b). In the diencephalon, *rbfox1* expression was detected in the
225 ventral habenular nucleus (HaV), in the anterior (A) and ventromedial (VM) thalamic nuclei (Figure
226 1B c). In the midbrain, *rbfox1* was detected in the posterior part of the parvocellular preoptic
227 nucleus (PPp, Figure 1B d), in the ventral zone of the periventricular hypothalamus (Hv, Figure 1B d,
228 e'), in the periventricular gray zone (PGZ,) and in the central zone (CZ) of the optic tectum (Figure 1B
229 e'), in the torus longitudinalis (TL) (Figure 1B e, e', g), in the periventricular nucleus of posterior
230 tuberculum (TPp), in the anterior tuberal nucleus (ATN, Figure 2B e, e''), in the posterior tuberal
231 nucleus of the hypothalamus (PTN, Figure 1B f) and in the paraventricular organ (PVO, Figure 1B f).
232 In the hindbrain, *rbfox1* was observed in the lateral division of the valvula cerebelli (Val) (Figure 1B
233 g).

234

235 ***rbfox1* mutant larvae show elevated cortisol levels and altered expression of *crhb*, *nr3c2*, *bdnf* and**
236 ***trkb2***

237 As RBFOX1 has been linked to regulation of HPA axis and *BDNF/TRKB* gene expression[4,15,16], we
238 examined the expression of components of the HPI axis and of *bdnf/trkb2.* In parallel, we measured
239 whole-body cortisol levels, in resting physiological conditions, at both larval and adult stages to
240 assess physiological outcomes. Since we did not observe significant differences in behaviour
241 between wild type and heterozygous animals, we employed wild type and homozygous animals only.

242 We performed qPCR experiments in 5dpf zebrafish larvae to assess changes in the expression levels
243 of the HPI axis markers corticotropin releasing hormone (*crhb*), mineralocorticoid receptor (*nr3c2*),
244 glucocorticoid receptor (*nr3c1*), corticotropin releasing hormone receptor 1 (*crhr1*), corticotropin
245 releasing hormone receptor 2 (*crhr2*), mineralocorticoid receptor 1 (*mc1r*), proopiomelanocortin a
246 (*pomca*), Krüppel-like factor 9 (*klf9*), as well as of *bdnf* and *trkb2*. In teleosts, the duplication of the
247 genome gave rise to two *CRH* genes, *crha* and *crhb,* and two *TRKB* genes, *trkb1* and *trkb2*[39,40]. Among
248 these, *crhb* and *trkb2* are most commonly referred to as the functional orthologues of mammalian
249 *CRH* and *TRKB* respectively, whereas *crha* and *trkb1* function appear more divergent and remain less
250 well understood [39,40]. Zebrafish also possess two *pomc* paralogues (*pomca* and *pomcb*) but only
251 *pomca* is functionally relevant for the activation of the HPI axis[41], and six melanocortin receptors
252 (*mc1r*, *mc2r*, *mc3r*, *mc4r*, *mc5ra*, *mc5rb*). Among these, we selected *mc1r* as representative of
253 melanocortin signalling. Then, unlike other teleosts, zebrafish possess a single copy of the *MR*

254 (*nr3c2*), *GR* (*nr3c1*) and *KLF9* (*klf9*) genes, and a single copy of the *BDNF* gene (*bdnf*)[40,42]. In
255 mammals, several *TRKB* splicing isoforms are present, but the most abundant ones are the full-
256 length (TRKB.FL/TK+) and the truncated (TRKB.T1/TK-), this latter lacking the catalytic tyrosine kinase
257 (TK) domain[43]. As in zebrafish the presence of both *trkb2* full-length and truncated forms has been
258 demonstrated[44], here we used a pair of *trkb2 TK+/TK-* common primers, and another pair targeting
259 only *TK+* to distinguish effects on the expression of the two isoforms.

260 In *rbfox1*$^{19del/19del}$ larvae, inwe observed a significant up-regulation of *bdnf* ($p < 0.05$) and *TK+* ($p <$
261 0.05), and a significant down-regulation of *TK-* ($p < 0.05$) expression levels (Figure 3A). Regarding HPI
262 axis, in *rbfox1*$^{19del/19del}$ larvae we found a significant up-regulation of *crhb* ($p < 0.0001$) and a
263 significant up-regulation of *nr3c2* ($p < 0.01$) (Figure 2B). We observed no significant changes in the
264 expression levels of the other genes examined ($p > 0.05$) (Figure 3B).

265 To assess *rbfox1* LoF effects on zebrafish larvae during early developmental stages, we performed
266 *crhb*, *bdnf* and *trkb2* qPCR experiments also in 3dpf larvae. Similarly to 5dpf larvae, in 3dpf
267 *rbfox1*$^{19del/19del}$ larvae we observed a significant up-regulation of *crhb* ($p < 0.01$), *bdnf* ($p < 0.05$) and
268 *TK+* ($p < 0.05$), and a significant down-regulation of *TK-* ($p < 0.05$) (Supplementary Figure 4A).

269 We measured whole-body cortisol levels under resting physiological conditions in both larvae and
270 adult zebrafish to evaluate the physiological impact of *rbfox1* loss and observed changes in *crhb*
271 expression. We found a significant increase in cortisol levels in *rbfox1*$^{19del/19del}$ larvae ($p < 0.05$)
272 (Figure 3C). In contrast, we observed no significant differences in adult fish ($p > 0.05$) (Figure
273 3C).These findings showed that *rbfox1* LoF led to alterations in stress-related gene expression and
274 cortisol levels in larvae, in line with our behavioural data and implicating *RBFOX1* as a critical
275 regulator of stress response mechanisms.

276 **Pharmacological treatment targeting TrkB signalling restores *crhb* and *nr3c2* gene expression and**
277 **disrupted hyperactivity, startle response and habituation in *rbfox1* LoF larvae**

278 To assess whether molecular and behavioural changes seen in *rbfox1* LoF larvae were mediated by
279 bdnf/trkb2 signalling, we repeated qPCRs and behavioural experiments in 5dpf zebrafish larvae
280 following chronic exposure (from 5 h to 5dpf) to the TRKB agonist 7,8-DHF or antagonist ANA-12. As
281 in our line *rbfox1* expression was knocked down throughout development, we initiated TRKB drug
282 treatment from gastrulation.

283 In *rbfox1*$^{+/+}$ larvae, neither TRKB agonist 7,8-DHF or antagonist ANA-12 had a significant effect on
284 *crhb* and *nr3c2* gene expression ($p > 0.05$) (Figure 3D, E). In *rbfox1*$^{19del/19del}$ larvae, chronic exposure
285 to either TRKB agonist or antagonist significantly reduced *crhb* and *nr3c2* expression levels relative
286 to untreated mutant larvae ($p < 0.001$), restoring gene expression to levels comparable with wild
287 type controls ($p > 0.05$) (Figure 3D, E). Following identification and removal of outliers (1 outlier in
288 the *rbfox1*$^{+/+}$ + ANA-12 group, 1 outlier in the *rbfox1*$^{+/+}$ + 7,8-DHF group and 1 outlier in the
289 *rbfox1*$^{19del/19del}$+ 7,8-DHF group), we observed a significant down-regulation of *nr3c2* expression
290 levels in *rbfox1*$^{19del/19del}$ + ANA-12 versus *rbfox1*$^{+/+}$ un-exposed controls ($p < 0.01$) (Figure 2D) and a
291 significant up-regulation of *nr3c2* expression levels in *rbfox1*$^{19del/19del}$+ 7,8-DHF versus both exposed
292 ($p < 0.01$) and un-exposed ($p < 0.05$) controls (Figure 3D, EE). Interestingly, while having the same
293 effect on *crhb* and *nr3c3* expression, ANA-12 and 7,8-DHF had different outcomes on *bdnf*
294 expression. Chronic treatment with ANA-12 reduced *bdnf* expression in *rbfox1*$^{+/+}$ ($p < 0.05$) but had
295 no effect on *rbfox1*$^{19del/19del}$. On the other hand, chronic treatment with 7,8-DHF increased bdnf levels
296 in both *rbfox1*$^{+/+}$ and *rbfox1*$^{19del/19del}$ larvae (Supplementary Figure C).

297 Then, we examined the effects of ANA-12 and 7,8-DHF on behaviour to assess which behavioural
298 alterations observed in *rbfox1* mutant were influenced by bdnf/trkb2 signalling. In presence of 7,8-

299 DHF we found a significant two-way interaction between genotype and drug on distance travelled
300 [Effect of genotype by drug: $\chi2(2) = 47.3782$, $p < 0.05$] and on swimming velocity [Effect of genotype
301 by drug: $\chi2(2) = 31.3951$, $p < 0.05$] such that treatment with 7,8-DHF restored hyperactive
302 behaviour observed in *rbfox1*$^{19del/19del}$ larvae ($p < 0.01$) (Figure 3F, G). Further, following chronic
303 exposure to 7,8-DHF there was no significant difference between *rbfox1*$^{19del/19del}$ and *rbfox1*$^{+/+}$ larvae
304 in response to startle with white light (Figure 3H) or in the proportion of responders to the acoustic
305 startle ($p > 0.05$) (Figure 3 I). ANA-12 had no significant effects on *rbfox1*$^{19del/19del}$ behavioural
306 alterations.

307 As the hypothalamus is the primary player in the stress response and Rbfox1 had only previously
308 been shown to affect TRKB expression within the hippocampus[16], we used ISH to determine whether
309 *trkb2* mRNA expression was reduced within the hypothalamic area. In agreement with previous
310 findings[45], in *rbfox1*$^{+/+}$ we found that *trkb2* is widely expressed in the brain of 5dpf larvae, whereas in
311 *rbfox1*$^{19del/19del}$ larvae, consistently with our qPCR experiments, we found a significant overall
312 reduction of *trkb2* mRNA in the whole brain (Figure 3J-L), including in the hypothalamus ($p < 0.01$)
313 (Figure 3M, N, P, Supplementary Figure 5).Our findings showed that the dysregulation in *crhb* and
314 *nr3c2* expression caused by *rbfox1* LoF was prevented by TRKB agonists and antagonists. Further, we
315 showed that hyperactivity, startle hypersensitivity and heightened proportion of responders to the
316 acoustic startles observed in *rbfox1* mutants are at least partially mediated by disrupted bdnf/trkb2
317 signalling.

318 ***rbfox1* LoF alters *pac1a* expression levels of zebrafish larvae**

319 As RBFOX proteins have been shown to be able to regulate *Pac1* alternative splicing to include the
320 *hop* cassette[7] and PAC1 has been shown to regulate *Bdnf* transcription and potentiate TRKB
321 activity[17], we examined expression levels of *pac1a,* the zebrafish homologue of the mammalian
322 *PAC1*, in *rbfox1*$^{+/+}$ and *rbfox1*$^{19del/19del}$ 5dpf larvae by qPCR.
323
324 In mammals there are several PAC1 isoforms and their role in the regulation of stress is poorly
325 understood[9]. In the brain, the predominant isoforms are *PAC1-hop* (long isoform) and *PAC1-short*[9].
326 Zebrafish possess two *pac1* genes, *pac1a* and *pac1b*, but only *pac1a* contains the *hop* cassette[9].
327 *PAC1-short* enhances *CRH* transcription, while *PAC1-hop* reduces *CRH* synthesis during late stress
328 recovery phase[4]. We measured expression levels of both *pac1a-short* and *-hop* isoforms and we
329 observed no differences in *pac1a-short* expression, but we found a significant up-regulation of
330 *pac1a-hop* in *rbfox1*$^{19del/19del}$ mutant larvae ($p < 0.05$) (Figure 3Q).

331 This finding shows that elevated pac1a-hop/Pac1a-hop alone is not sufficient to counteract *crhb*
332 increase and strengthens previous data[7] suggesting that RBFOX1 is not the main regulator (or at
333 least not the sole regulator of) *PAC1* alternative splicing..

334 ***rbfox1* mutants undergo adaptive mechanisms and allostatic overload during development**

335 The HPA axis possesses a vital role in the maintenance of allostasis, the process by which the body
336 achieves stability in response to stress or environmental challenges. Dysregulation of the HPA axis
337 often leads to disrupted allostasis during later life, also termed as allostatic load (i.e., the
338 physiological consequence resulting from the cumulative "wear and tear" of the body in response to
339 chronic stress)[22]. As we observed dysregulation of the HPI axis gene expression in *rbfox1* mutant
340 larvae and altered behavioural responses in *rbfox1* mutant larvae but not in adults, we assessed
341 expression of HPI axis components in adult zebrafish, in the presence and absence of acute stress
342 (NTD), to explore the possibility of adaptation that may contribute to differences in allostatic load.

343 We first measured *crhb*, *nr3c2*, *nr3c1*, *bdnf* and *trkb2* mRNA expression levels. In physiological
344 resting conditions, we observed no differences in HPI nor *bdnf/trkb2* expression levels ($p > 0.05$)

345 (Figure 4A, B). However, after stress exposure, regarding the HPI axis, in *rbfox1*$^{19del/19del}$ adults we
346 observed the same dysregulation seen in *rbfox1* LoF larvae: we found significant up-regulation of
347 *crhb* ($p < 0.001$) and *mr* ($p < 0.0001$) and no changes in *nr3c1* expression levels ($p > 0.05$) (Figure 4A),
348 and significant up-regulation of *bdnf* ($p < 0.01$) and *TK+* ($p < 0.05$), and significant down-regulation of
349 *TK-* ($p < 0.05$) (Figure 4B, C).

350 Excess glucocorticoid (GC) exposure during early developmental stages or early life stress (ELS) can
351 lead to vulnerability to allostatic overload in the long-term[19,22]. One of the effects caused by GC- or
352 ELS-induced allostatic overload is reduced cell proliferation during adulthood[19]. This effect has been
353 suggested to be developmentally dynamic, since it is often preceded by increased cell proliferation
354 during early stages[19]. Further, BDNF signalling has been shown to regulate neural stem cell
355 proliferation through TK-, suggesting that *rbfox1* LoF fish showing altered levels of *TK-* expression,
356 may show altered proliferation across the life course[46]. We therefore assessed the rate of
357 proliferation at both larval and adult stages using qPCR for proliferating cell nuclear antigen (*pcna*).
358 We observed a significant up-regulation of *pcna* expression levels in 5dpf *rbfox1*$^{19del/19del}$ zebrafish
359 larvae ($p < 0.05$) and a significant down-regulation of *pcna* expression levels in the brains of adult
360 *rbfox1*$^{19del/19del}$ fish ($p < 0.01$) when compared to *rbfox1*$^{+/+}$ siblings (Figure 4D).

361 In adult zebrafish, other effects caused by GC-induced allostatic overload include reduced fertility
362 and survival rates[19]. Therefore, we assessed fertility and survival of *rbfox1*$^{19del/19del}$ zebrafish and
363 *rbfox1*$^{+/+}$ siblings. We found that both fertility ($p < 0.05$) and survival ($p < 0.001$) rates of
364 *rbfox1*$^{19del/19del}$ fish were significantly reduced compared to *rbfox1*$^{+/+}$ siblings (Figure 4E, F).

365 Consistent with our findings (disrupted HPI axis gene expression and increased cortisol in *rbfox1*
366 mutant larvae under resting physiological conditions and in *rbfox1* adult mutant only following stress
367 exposure), these results suggest that *rbfox1* mutants may engage compensatory mechanisms during
368 development similar to those triggered by early-life GC exposure. While these mechanisms may
369 transiently restore homeostasis, they likely lead to enduring alterations in stress responsivity and
370 neurodevelopmental trajectories.

371 **DISCUSSION**

372 In this study we generated a CRISPR-Cas9 LoF *rbfox1* zebrafish line (*rbfox1*^{19del}) to investigate the
373 mechanisms by which *RBFOX1* LoF increases susceptibility to psychiatric disorders.
374
375 Allostatic load has been linked with several cognitive disorders including depression, schizophrenia,
376 anxiety and PTSD[47]. HPA axis overactivity is a key factor in the onset of the allostatic load[22]. RBFOX1
377 has been shown to influence expression of stress-related genes such as PAC1 and BDNF/TRKB.
378 Therefore, alterations in RBFOX1 function may increase psychiatric disorder vulnerability through
379 alterations in stress response systems, such as the HPA axis, pre-disposing to allostatic overload
380 vulnerability in later life (Figure 5).
381
382 Similarly to *Rbfox1* deficient mice[6] and as seen in previous studies employing *rbfox1* mutant
383 zebrafish[2,23], we found that *rbfox1*$^{19del/19del}$ mutants were hyperactive and impulsive. These findings
384 are consistent with studies implicating common and rare *RBFOX1* genetic variants as risk factors for
385 psychiatric disorders like ASD, ADHD, schizophrenia and anxiety/stress disorders[5,6,48]. At larval stages
386 *rbfox1*$^{19del/19del}$ were hyperactive and had increased burst swimming, indicative of increased
387 impulsivity. In the response and habituation to acoustic startle assay, *rbfox1*$^{19del/19del}$ larvae startled
388 more and had a higher response rate over time compared to *rbfox1*$^{+/+}$ siblings, consistent with
389 previous findings in *rbfox1* mutant zebrafish[30]. In a forced light-dark assay, although baseline
390 hyperactivity of *rbfox1*$^{19del/19del}$ larvae makes interpretation difficult, *rbfox1*$^{19del/19del}$ larvae showed an
391 increased startle response upon dark to light transition, consistent with heightened anxiety. These

392 results suggest that *rbfox1* LoF leads to heightened arousal, aligning with studies linking *RBFOX1* to
393 mood and anxiety disorders, including PTSD[49]. Interestingly, *rbfox1* $^{19del/19del}$ adults showed reduced
394 bottom dwelling only during the first minute of the novel tank diving assay (an adult measure of
395 anxiety-like behaviour) while there were no significant differences during the remaining 4 minutes of
396 the assay This latter result suggests behavioural adaptation possibly coupled with increased
397 impulsivity or impaired threat assessment (decreased bottom dwelling during the first minute of
398 assay. This aligns with the broader *rbfox1*$^{19del/19del}$ behavioural profile (hyperactivity, heightened
399 startle and poor habituation at larval stages) indicative of dysregulated arousal rather than reduced
400 anxiety. Similarly, in the 5-CSRTT we found that *rbfox1*$^{19del/19del}$ were more impulsive than *rbfox1*$^{+/+}$
401 siblings, consistent with *RBFOX1* variants being associated with impulsivity and related disorders
402 such as ADHD and ASD[6].
403
404 In *rbfox1* LoF larvae, under resting physiological conditions, we observed increased cortisol levels
405 and dysregulation of *crhb* and *nr3c2*, both key components of fish HPI axis, which is analogous to the
406 HPA axis in mammals. The HPA axis is crucial for managing stress, with CRH triggering cortisol
407 secretion, affecting metabolism, immunity, and behaviour[50,51]. In zebrafish larvae under resting
408 physiological conditions, we found increased cortisol, *crhb* and *nr3c2*, with no changes in the
409 expression levels of the other HPI axis genes assessed (*nr3c1*, *crhr1*, *crhr2*, *mc1r*, *pomca*, *kf19*). In
410 adults, although resting levels were unchanged, *rbfox1* LoF showed an exaggerated molecular
411 response to stress. Notably, both CRH and MR have important roles in the brain beyond their
412 canonical endocrine functions via the HPA axis. CRH regulates anxiety and arousal acting as a
413 neuromodulator in limbic regions such as the amygdala and hippocampus[52]. Similarly, hippocampal
414 MRs play a key role in early stress responses by supporting cognitive appraisal of novel situations
415 and promoting behavioural flexibility, thus shaping the initial reaction to stress[53]. Elevated cortisol
416 and *crhb* levels as seen in *rbfox1*$^{19del/19del}$ larvae under resting physiological conditions, suggest a
417 chronic anxiety state. Increased cortisol, CRH and MR levels are linked to mood disorders like
418 depression and PTSD[54–57]. These findings support a role for *RBFOX1* in *CRH* regulation and suggest
419 that *RBFOX1* LoF may contribute to mood disorders and stress resilience via HPA axis dysregulation
420 and/or non-canonical brain-specific effects of CRH and MR.
421
422 BDNF and TRKB are also key regulators of the stress response[58]. BDNF levels often increase during
423 stress to promote neuronal survival and plasticity, buffering negative effects of stress on the brain
424 via TRKB[10,11,13,58–60]. Dysfunction of BDNF/TRKB signalling is linked to several stress-related
425 disorders[13]. The increased *bdnf* expression we observed in *rbfox1*$^{19del/19del}$ larvae may suggest a
426 compensatory response to cope with *crhb* increase and maintain homeostasis. Given BDNF's
427 established role in modulating neuronal plasticity and stress adaptation, its upregulation may serve
428 to stabilise or buffer hypothalamic circuits disrupted by excessive *crhb* transcription[58]. This response
429 could represent an intrinsic attempt to mitigate possible overactivation of the HPI axis or the
430 reduced activity within the trkb2 signalling (a suggestion supported by finding that incubation in the
431 TRKB agonist 7,8-DHF rescues the behaviour as well as the expression of *crhb*) and maintain
432 functional equilibrium in the face of impaired regulatory input caused by *rbfox1* loss. Alternatively,
433 the observed increase in *bdnf* expression could result from either dysregulation of BDNF repressors
434 or an imbalance in TRKB isoform expression caused by RBFOX1 loss, where upregulation of the full-
435 length isoform may enhance BDNF expression through a positive feedback mechanism[40,61]. At 3 and
436 5dpf, in *rbfox1*$^{+/+}$ larvae we detected both *trkb2* truncated (*TK-*) and full-length (*TK+*) forms, and in
437 *rbfox1*$^{19del/19del}$ larvae we observed a significant down-regulation of *TK-* and a significant up-
438 regulation of *TK+*, which is predicted to lead to an increased activation of TRKB signalling, consistent
439 with the increased *crhb* expression as seen here[62]. Studies in rodents showed that *Rbfox1* up-
440 regulation led to increased TrkB.T1 (TK-) expression in the hippocampus and no changes were
441 observed following *Rbfox1* deletion[16]. In contrast, we observed down-regulation of *trkb2 TK-*
442 expression in *rbfox1*$^{19del/19del}$ larvae in resting physiological conditions. The difference between these

443 studies may be due to i) differences in the tissue examined (zebrafish larvae whole head versus
444 rodent hippocampus), ii) the developmental stage of the animals (larval versus adult stage), iii) the
445 genotype of the animals studied (*rbfox1*$^{19del/19del}$ in our study versus *Rbfox1*$^{+/-}$ in the study in rodents),
446 or iv) presence of compensatory mechanisms (in the hippocampal mouse model *Rbfox1* knockdown
447 resulted in up-regulation of *Rbfox2*). As for this latter hypothesis, as in previous studies in zebrafish[2],
448 we did not see any changes in *rbfox2* expression upon *rbfox1* LoF (Supplementary Figure4)
449 suggesting that this compensatory mechanism does not occur in larval fish.
450
451 Consistent with the possibility that *RBFOX1* LoF may contribute to dysregulation of the HPA axis
452 through a direct or indirect effect on BDNF/TRKB pathway, chronic exposure to TRKB agonist (7,8-
453 DHF) or antagonist (ANA-12) restored HPI axis gene expression to that seen in *rbfox1*$^{+/+}$ larvae. ANA-
454 12 is a selective non-competitive antagonist of TRKB exerting central TRKB blockade and producing
455 rapid and long-lasting anxiolytic and antidepressant effects[63]. Mice treated with ANA-12 showed
456 reduced anxiety-like behaviour[63] and in stressed rats, ANA-12 blocked *Crh* increase in the
457 hypothalamus and amygdala[64]. 7,8-DHF is a potent selective agonist of TRKB used in the treatment
458 of several disorders, including depression and schizophrenia, and has been shown to enhance
459 memory consolidation and emotional learning in healthy rodents[65]. In a similar fashion to the effects
460 of ANA-12 seen in rats (blocking *Crh* increase)[57], after chronic treatment with ANA-12, we observed
461 that the expression of HPI axis genes in *rbfox1*$^{19del/19del}$ larvae was restored to *rbfox1*$^{+/+}$ levels. [66]
462 Interestingly, ANA-12, despite restoring *crhb* and *nr3c2* levels to wild type, did not rescue
463 *rbfox1*$^{19del/19del}$ larvae behaviour, indicating that blockade of TRKB can normalise some aspects of HPI
464 axis output but is insufficient to correct the behavioural phenotype (perhaps because it further
465 disrupts necessary TRKB-mediated signalling in the brain). In contrast, 7,8-DHF, normalises *crhb* and
466 *nr3c2* expression and rescues some behavioural aspects altered in *rbfox1*$^{19del/19del}$ larvae (i.e.,
467 hyperactivity, startle response to white light stimulus and proportion of fish responding to acoustic
468 stimuli), suggesting that enhancing TRKB signalling through the full-length receptor may restore
469 functional signalling balance and downstream pathways (e.g., synaptic plasticity, habituation
470 mechanisms). Finally, the fact that 7,8-DHF increases *bdnf* expression in *rbfox1*$^{19del/19del}$ larvae while
471 ANA-12 has no effect suggests a potential positive feedback loop whereby TRKB activation enhances
472 BDNF expression, helping restore adaptive neuroendocrine and behavioral responses. Future studies
473 employing acute or temporally restricted treatments (e.g., 3–5 dpf), or employing different TRKB
474 agonist/antagonist, will help delineate the specificity of TRKB signalling effects. Interestingly,
475 *rbfox1*$^{19del/19del}$ larvae were differentially sensitive to the effect of TRKB drugs on *nr3c2* expression,
476 most likely due to the unbalanced *TK+/TK-* levels. These findings warrant further investigations. It is
477 of note that neither TRKB agonist nor antagonist had a significant effect on *crhb* nor *n3cr2*
478 expression in *rbfox1*$^{+/+}$ larvae. One possible explanation is that, as the larvae were not exposed to
479 any stressors, any effect on Trkb2 signalling had limited effect on HPI axis activity.

480
481 In *rbfox1*$^{19del/19del}$ larvae, we also observed up-regulation of *pac1a-hop* with no changes in *pac1a-*
482 *short* levels. Previous studies in zebrafish have shown that Pac1-short gain of function caused
483 persistent *crh* increase, while overexpression of Pac1-hop prevented stress-induced *crh* transcription
484 activation[4]. These previous studies also suggest that RBFOX1 regulates the alternative splicing of
485 *PAC1* promoting the formation of *PAC1-hop*[4]. However, the increase in *pac1-hop* seen in our study
486 argues against this suggestion and suggests an adaptive response to the increased expression of *crh*
487 either through *rbfox2*[7] (whose expression was not altered by *rbfox1* LoF (Supplementary Figure4)) or
488 through an unknown mechanism. Elevated *pac1a-hop*/Pac1a-hop alone might be not sufficient to
489 counteract *crhb* upregulation, given the concurrent increase in *bdnf* levels and the shift in *trkb2*
490 isoform expression (upregulation of the excitatory long form and downregulation of the inhibitory
491 short form). This interpretation is further supported by the decreased in *crhb* levels observed
492 following chronic TRKB modulation. Another option is that the upregulation of *pac1a-hop* mRNA
493 may not reflect increased functional Pac1a-hop receptor activity, particularly in the context of

494 disrupted splicing regulation following *rbfox1* loss, suggesting that RBFOX1 might be involved in
495 *PAC1* mRNA stability rather than alternative splicing.
496
497 In contrast to larvae, differences in HPI axis and *bdnf/trkb2* gene expression and cortisol levels were
498 not seen in adult animals under resting conditions. However, *rbfox1*$^{19del/19del}$ adults showed increased
499 *crhb* and *nr3c2* on challenge with a stressor, aligning with the previous suggestion that Rbfox1 is
500 required for the termination of the acute endocrine stress response[4] and that chronic stress during
501 development leads to adult HPI axis adaptation, often at a cost in later life (e.g., altered stress
502 responsivity, reduced fertility and survival, decreased *pcna* expression)[19,67]. This interpretation is
503 consistent with previous work by Eachus et al., which demonstrated that early-life exposure to
504 excess GC can lead to long-term changes in stress-regulatory circuits and adult behavioural
505 dysfunction[19]. Supporting this, *rbfox1* LoF adults show heightened *crhb*, *nr3c2* and *bdnf* expression,
506 and imbalance in *trkb2* isoform expression, specifically in response to a stressor (the novel tank
507 diving assay). Together, these findings suggest that while baseline homeostasis may be restored
508 through developmental adaptation, stress responsivity remains dysregulated, pointing to an
509 allostatic shift toward a passive coping style for *rbfox1* mutants[68,69]. Passive (cautious, risk-averse,
510 high CRH) and active (bold, exploratory, low CRH) coping styles refer to behavioural strategies that
511 animals employ to respond to stress and that are underpinned by distinct neuroendocrine pathways,
512 providing a valuable framework for interpreting stress susceptibility, resilience and the behavioral
513 consequences of genetic mutations[68,69]. The shift toward a passive coping style of *rbfox1* mutants
514 support a role for RBFOX1 in shaping stress responsivity and behavioural strategies. In *rbfox1*$^{19del/19del}$
515 adults we observed also reduced fertility and reduced survival rates, two long-term effects often
516 associated with excess GC-exposure/early life stress[19]. Another long-term effect of excess GC-
517 exposure/early life stress is reduced neural stem cell proliferation in adult animals, often
518 accompanied by increased proliferation at early stages[19]. Our findings that *rbfox1*$^{19del/19del}$ showed
519 increased *pcna* levels at larval staged but reduced *pcna* levels during adulthood, corroborate this
520 latter hypothesis of a dynamic developmental effect of early life stress. Consistent with the *crhb*
521 increase observed in stressed *rbfox1*$^{19del/19del}$ adults, and as seen in larvae, after acute stress,
522 *rbfox1*$^{19del/19del}$ adults also showed unbalanced *trkb2* expression, with up-regulation of *TK+* and down-
523 regulation of *TK-* .
524
525 In conclusion, given the conservation between fish HPI axis and the mammalian HPA axis, our data
526 unveils a pivotal new finding in *CRH* regulation, revealing an interplay between RBFOX1 and
527 BDNF/TRKB in the context of chronic stress and stress resilience and suggests that RBFOX1 plays a
528 crucial role in adaptive stress mechanisms. In response to stressful challenges, RBFOX1 functions as a
529 "switch" regulating the balance between short/long isoforms of TRKB receptors: during the stress
530 recovery phase, RBFOX1 switches the balance towards *TRKB.T1/TK-* isoform, decreasing *CRH* levels
531 and turning off the HPA axis (Figure 5). In *rbfox1*$^{19del/19del}$, this regulatory switch appears disrupted
532 (increased cortisol, *crhb*, *nr3c2*, *bdnf*, and full-length *trkb* expression alongside reduced truncated
533 *trkb*) suggesting a failure to terminate the stress response. Behaviourally, mutants exhibited
534 hyperactivity, impulsivity, heightened arousal, and reduced habituation, phenotypes that parallel
535 core symptoms seen in several human psychiatric disorders. Pharmacological experiments support a
536 functional consequence of this dysregulation. Although both ANA-12 (TRKB antagonist) and 7,8-DHF
537 (TRKB agonist) normalised *crhb* and *nr3c2* levels, only 7,8-DHF rescued behavioural abnormalities.
538 These findings suggest that restoring balanced TRKB signalling (by selectively enhancing the activity
539 of residual inhibitory TRKB.T1 receptors without compromising the beneficial effects mediated by
540 excitatory TRKB.FL receptors) is critical for functional recovery. This supports the idea that an
541 imbalance in TRKB isoform expression, rather than overall receptor activity, may underlie the
542 observed behavioural pathology. The differential effects of these compounds also point to a possible

role for positive feedback in BDNF expression via TRKB-FL signalling, which may be essential for behavioral homeostasis. Together these results suggest that *RBFOX1* contributes to the liability of psychiatric disorders through CRH, MR and BDNF/TRKB dysregulation, which leads to disrupted development and vulnerability to allostatic overload in later life. The suite of behavioural effects seen in *rbfox1* LoF animals coupled with exaggerated response on exposure to a stressor are reminiscent of reported traits in passive versus active coping styles[68] suggesting that RBFOX1 activity may also play a key role in individual differences in coping strategies. Although we show a key role for RBFOX1 in regulation of the HPA axis, consistent with this being a primary mechanism by which *RBFOX1* variants pre-disposes to psychiatric disorders, RBFOX1 regulates the splicing of a wide range of additional genes[15] which may also play a part of disease vulnerability.

METHODS

Animal maintenance

All fish were maintained in a recirculating system (Tecniplast, UK) with a 14h:10h light/dark cycle and a constant temperature of 28°C. Fish were fed with ZM-400 fry food (Zebrafish Management Ltd.) in the morning and brine shrimps in the afternoon. Breeding was set up in the evening, in sloping breeding tanks (Tecniplast) provided with dividers for timed mating. The following morning, dividers were removed to allow spawning. Eggs were collected in Petri dishes (max 50 eggs/dish). Infertile eggs were removed, and fertile ones were incubated at 28°C. Petri dishes were checked daily to ensure consistent developmental stage across groups. If reared, larvae were moved to the recirculating system at 5 days post fertilization (dpf) and fed as stated above.

All procedures were carried out under license in accordance with the Animals (Scientific Procedures) Act, 1986 and under guidance from the Local Animal Welfare and Ethical Review Board at Queen Mary University of London.

Although our previous studies examined two distinct *rbfox1* mutant lines (*rbfox1*^{del19} vs *rbfox1*^{sa15940})[2], we chose to focus on the *rbfox1*^{del19} line for the current study due to its more pronounced phenotype.

Generation of *rbfox1* loss of function zebrafish line

The zebrafish *rbfox1* loss of function (LoF) mutant line was generated as described previously using Tübingen strain as background [71]. CRISPR RNA (crRNA) (Merck) was designed to target *rbfox1* exon 2 (**CCC**AGTTCGCTCCCCCTCAGAAC, PAM sequence in bold, MwoI recognition site underlined). A 3 µL injection mix containing 1 µL (F_C 83 ng/µL) crRNA, 1 µL (F_C 83 ng/µL) tracrRNA (Merck, #TRACRRNA05N), 1 µL (F_C 1.67 µM) and 1 µL Cas9 protein (New England Biolabs, #M0646) was freshly prepared on the morning of the injection procedure. Then, 1 nL of the injection mix was injected into one-cell stage zebrafish embryos (~ 100-150 embryos). Injection efficacy was assessed at 24 hours post fertilization (hpf) by polymerase chain reaction (PCR) from genomic DNA (*rbfox1*_Forward, 5′-TAATCAAGACGCCCCAGCAC–3′; *rbfox1*_Reverse, 5′-GTACTCAGCAGGAATGCCGT- 3′) followed by MwoI (New England Biolabs, #R0573S) restriction enzyme digestion. Successful injections will introduce indel mutations disrupting the recognition site of the restriction enzyme, preventing this latter from cutting the PCR amplicon. Once reached sexual maturity (at ~ 3 months of age) injected fish (F_0) were outcrossed with wild type to generate F_1 embryos. The progeny may carry different mutations due to the mosaic nature of the F_0 parents. F_1 fish were therefore screened for mutations leading to premature termination codon (PTC) via cloning into pGEM-T Easy vector (Promega, #A1360), followed by transformation, colony PCR, DNA

588 purification (Monarch® Plasmid Miniprep Kit, New England Biolabs, #T1010) and sequencing (Source
589 BioScience PLC). Quantitative real time PCR (qPCR) was used to confirm reduction of *rbfox1* mRNA
590 expression.
591
592 **Fish breeding and genotyping**
593
594 For adult experiments, mixed sexes were used. When possible, animals were associated with an
595 identification number and genotype was assigned after data analysis. For larval experiments, fish
596 were generated by heterozygous in-cross and genotyped prior to data analysis. Genomic DNA was
597 extracted from fins and using the HotSHOT method. Briefly, samples were incubated at 95 °C in 50
598 mM NaOH for 30 min, followed by 1 min at 10 °C. Reaction was stopped using 1M Tris HCl (1/10 of
599 the initial NaOH volume), pH 8.00. Genotyping primers were the same as the ones used to identify
600 founder carriers.
601
602 **Drug Treatment**
603
604 Zebrafish embryos of each genotype (*rbfox1*$^{+/+}$ and *rbfox1*$^{19del/19del}$) were treated from 5hpf to 5dpf
605 with 20 µM TRKB antagonist ANA-12 (abcam, Cat.ab146196), or 20 µM TRKB agonist 7,8-
606 dihydroxyflavone (7,8-DHF) (abcam #ab120996), or dimethylsulfoxide (DMSO, vehicle 0.01%) (Merck
607 #34869). Treatment was performed in Petri dishes (max 30 embryos x dish) and drugs or vehicle
608 were dissolved in fish water. Solutions were replaced daily.
609
610 **Quantitative Real-Time PCR**
611 Quantitative Real-time PCR (qPCR) of target RNA was performed on 5dpf *rbfox1* wild type (*rbfox1*$^{+/+}$)
612 and *rbfox1* homozygous (*rbfox1*$^{19del/19del}$) larvae, using Luna® Universal One-Step RT-qPCR Kit (New
613 England Biolabs #M3005) and a Bio-Rad 96-well qPCR machine (CFX96 Touch Real-Time PCR
614 Detection System). Total RNA was isolated using TRIzol reagent (Thermo Fisher Scientific) following
615 manufacturer's instructions. Briefly, after homogenization, RNA was isolated by precipitation, rinsed
616 in ethanol and resuspended in RNase free water. Total RNA was then quantified using BioDrop
617 (Biochrom Ltd.), and up to 1 µg was reverse transcribed to cDNA using the ProtoScript II First Strand
618 cDNA Synthesis Kit (New England Biolabs, #E6560) following manufacturer's instructions. The
619 resulting cDNA yield and quality were evaluated using BioDrop (Biochrom Ltd.). As for zebrafish
620 *trkb2 TK+* and *TK-* isoforms quantification, Ct values resulting from the amplification of the *TK+*
621 specific product were subtracted from the Ct values resulting from the amplification of the *TK+/TK-*
622 common product. All reactions included 5 biological replicates and 3 technical replicates. For
623 experiments in larvae, each biological replicate consisted of 15 larval heads (eyes and jaw removed).
624 For experiments in adults, each biological replicate consisted of a single brain. Actin – β 2 (*actb2*) and
625 ribosomal protein L13a (*rpl13a*) were employed as reference genes. For assessing *rbfox1* mRNA
626 expression, *rbfox1* primers were designed upstream of the CRISPR deletion. Accession numbers,
627 primer sequences and amplification efficiencies for all the reference and target genes can be found
628 in Supplementary Table 1.
629
630 ***In situ* hybridization**
631 *In situ* hybridization (ISH) was carried out on whole mount zebrafish larvae and on larval (sagittal)
632 and adult brain (transverse) sections as described previously[2]. For *rbfox1* ISH, the original plasmid
633 used to generate the riboprobe was provided by Dr William Norton (University of Leicester). The
634 plasmid used to produce the *trkb2* riboprobe was generated in our laboratory (Forward primer: 5'-

635 GTTCGTGGAATGGCTTGCTG-3', Reverse primer: 5'-TCTGGCCCACGATGTTTTCA-3') using the pGEM®-T
636 Easy Vector System (Promega, #A1360) and *in-house* generated *E. coli* DH5α competent cells.
637 Riboprobes to identify *rbfox1* (NM_001005596) and *trkb2* (NM 01197161.2) mRNA were synthetized
638 by *in vitro* transcription (IVT) using MAXIscript™ SP6/T7 kit (Invitrogen by Thermo Fisher Scientific,
639 #AM1322), following manufacturer's instructions and using a DIG RNA Labeling Mix, 10× conc
640 (Roche, #11277073910) containing digoxigenin labeled uracil.
641
642 *In situ* hybridization on whole mount zebrafish larvae
643
644 *In situ* hybridization was carried out on 28hpf, 2- 3- 4- and 5dpf *rbfox1*$^{+/+}$ and *rbfox1*$^{19del/19del}$ larvae.
645 To prevent skin pigmentation, embryos were incubated in 0.2 mM 1-phenyl 2-thiourea (PTU) (Sigma,
646 #S527335) from 24hpf. When they reached the desired age, larvae were fixed in 4%
647 paraformaldehyde (PFA) (Merck, #158127) overnight (ON) at 4°C. The following day, larvae were
648 rinsed in 1x phosphate buffered saline (PBS) (Thermo Fisher Scientific, #18912014) supplemented
649 with Tween 20 (Sigma, #P1379) (0.05% v/v), dehydrated in ascending methanol series (25%, 50%,
650 70%, 80%, 90%, 100% methanol, 5 min each) and stored in 100% methanol at -20 °C. To perform ISH
651 experiments, larvae were rehydrated in descending methanol series (100%, 90%, 80%, 70%, 50%,
652 25% methanol), 5 min each, and washed in 1xPBS, 5 min. Larvae were permeabilized using
653 proteinase K (PK) (ITW Reagents, #A3830) (stock 20 µg/mL in 1xPBS) as follows: 28hpf larvae were
654 permeabilized in PK 1:2000 in 1xPBS for 20 min at room temperature (RT), older stages were
655 permeabilized in PK 1:1000 at 37°C for at least 30 min. Then, larvae were post fixed in 4% PFA for 20
656 min and washed in 1xPBS at RT, 5 x 5 min. Prehybridization was carried out in hybridization solution
657 (HB) containing 50% formamide, 5% saline sodium citrate buffer (SSC), 50 µg/mL heparin, 0.05
658 mg/mL yeast RNA, 0.1% Tween 20, and 0.92% citric acid at 68 °C for 2h. Thereafter, larvae were
659 incubated in HB containing *rbfox1* riboprobe (500 pg/µL), ON at 68°C. Post hybridization washes
660 were performed at 68°C with a gradient of 2xSSC and formamide (50%, 25% and 0% formamide), 10
661 min each, and then twice with 0.02xSSC, 30 min each. Subsequently, larvae were blocked in blocking
662 solution (BS) containing 10% normal sheep serum (Gibco, #16070096) and 2 µg/µL bovine serum
663 albumin, for 1h at RT. After blocking step, larvae were incubated in anti-digoxigenin Fab fragments
664 conjugated with alkaline phosphatase (Roche, #11093274910), 1:2000 in BS, 1h at RT and then ON
665 at 4°C. The following day, larvae were washed in 1xPBS, 6 x 15 min each, and then in alkaline
666 phosphatase (100 mM NaCl, 100 mM Tris HCl, 50 mM MgCl2, 0.1% Tween 20) (NTMT) buffer, 3 x 5
667 min each. The chromogenic reaction was carried out by incubating the larvae in BCIP/NBT solution
668 (Merck, #203790) in NTMT buffer, at RT in the dark, and were observed every 20 min until the signal
669 detection. After reaching the desired staining, larvae were washed in 1xPBS at RT, post fixed in 4%
670 PFA for 2h, cleared and stored in 80% glycerol at 4°C. For sagittal cryosections, larvae were
671 embedded in 1.5% low gelling temperature agarose (Scientific Laboratories Supplies, #A9414)
672 supplemented with 5% Sucrose in 1xPBS. Sections (5 µm) were collected on adhesive microscope
673 slides Superfrost® Plus Gold (Epredia).
674
675 *In situ* hybridization on sections
676
677 ISH was conducted on paraffin embedded *rbfox1*$^{+/+}$ and *rbfox1*$^{19del/19del}$ adult brains (transverse
678 sections) and 5dpf *rbfox1*$^{+/+}$ and *rbfox1*$^{19del/19del}$ zebrafish larvae (sagittal sections). Fish were culled by
679 an overdose of tricaine prior to head removal. Dissected adult brains and larvae were fixed in 4%
680 PFA in 1xPBS, ON at 4°C. Tissues were then rinsed in 1xPBS and dehydrated in ascending ethanol
681 series (15 min in each of 30%, 50%, 70%, 80%, 90%, 100% ethanol) and embedded in paraffin.
682 Transverse (adult brains) or sagittal (5 days old larvae) sections of 12 µm (adult brains) or 7 µm (5

683 days old larvae) thickness were cut using a microtome (Leica). To perform ISH, slides were de-waxed
684 in xylene (twice, 10 min each), rehydrated in descending ethanol series (2 x 5 min in absolute
685 ethanol, then 90%, 80%, 70%, 50% and 25% ethanol, 5 min each), and rinsed in 1xPBS for 5 min.
686 Then, sections were permeabilized using PK (0.05 µg/µL) for 8 min at RT, washed with 2 mg/mL
687 glycine twice (5 min each), post fixed in 4% PFA for 20 min and washed in 1xPBS at RT.
688 Prehybridization was carried out in HB, for 1h at 68°C. Thereafter, sections were incubated in HB
689 containing *rbfox1* riboprobe (500 pg/µL), ON at 68°C. Post hybridization washes were performed at
690 68°C twice for 20 min in 1xSSC, twice for 20 min in 0.2xSSC, and several washes were performed in
691 1xPBS, 5 min each at RT. Then, sections were blocked in BS for 30 min at RT and incubated in a
692 1:2000 dilution of anti-digoxigenin Fab fragments conjugated with alkaline phosphatase in BS, ON at
693 4°C. The following day, sections were washed in 1xPBS, 5 x 10 min each. The chromogenic reaction
694 was carried out by incubating the slides in BCIP/ NBT solution in NTMT buffer, at RT in the dark, and
695 were observed every 20 min until the signal detection. When the desired staining was obtained,
696 sections were washed in 1xPBS at RT, dehydrated in ascending ethanol series (25%, 50%, 70%, 80%,
697 90%, 100% ethanol, 5 min each), cleared in xylene (twice, 5 min each) and mounted with dibutyl
698 phthalate polystyrene xylene mounting medium (Sigma, #06522).

699 **Image acquisition and processing**

700 Pictures of whole mount ISH on zebrafish larvae were acquired by Leica MZ75 microscope. For ISH
701 on sections, pictures were acquired using a Leica DMRA2 upright epifluorescent microscope with
702 colour QIClick camera (Leica) and processed with Velocity 6.3.1 software (Quorum Technologies Inc).
703 Quantification of the ISH staining signal intensity was performed as described previously[72], using Fiji
704 software[73]. Adult anatomical structures were identified according to the Neuroanatomy of the
705 Zebrafish Brain by Wullimann [74].

706 **Behavioral Assays**

707 For larvae, all behavioural experiments were conducted on the progeny of a *rbfox1*$^{+/19del}$ in-cross.
708 Larvae were genotyped prior to data analysis. For adults, where the genotype of the animals was
709 known, fish were pseudorandomised across testing systems with all trials having an approx. equal
710 number of each genotype. The adult fish were weight- and age-matched, with approximately equal
711 numbers of both sexes. Sex was not treated as a biological variable in the statistical analyses.

712

713 Larval behavioural experiments

714 Patterns of locomotor activity of 5dpf *rbfox1*$^{+/+}$, *rbfox1*$^{+/19del}$ and *rbfox1*$^{19del/19del}$ mutant zebrafish
715 larvae were investigated as described previously[24,29,33]. Tests were conducted between 9 a.m. and 4
716 p.m. At 5 dpf, larvae were placed in individual wells of a 24-well plate. To reduce stress due to
717 manipulation, larvae were acclimatised for at least 1 h before testing. Then, plates were placed into
718 the DanioVision observation chamber (Noldus). Locomotion parameters such as distance travelled
719 and swimming velocity were recorded using EthoVision XT software (Noldus). Data were exported in
720 1 min and 1 sec time bins and analysed with R programming language[75]. For the hyperactivity assay,
721 larval basal locomotion was tracked for 15 min in dark conditions. Larval swimming burst was
722 assessed as described previously[24] and peaks were considered as the acceleration events when
723 larvae travelled > 5 mm in < 12 sec. The forced light-dark transition assay was performed as
724 described previously[76,77] with modifications: after an initial 5 min period of dark (baseline), larvae
725 were exposed to one light/dark cycle of 1 min light (Noldus white light device) followed by 5 min

726 dark. The response and habituation to acoustic startle stimuli was performed as described
727 previously[29]: after 10 min of baseline (no stimuli, dark conditions), larvae were subjected to 10
728 sound/vibration stimuli (Noldus tapping device) over 20 sec (2 sec intervals between each stimulus).

729 5-Choice Serial Reaction Time Task

730 We measured impulsive action using a zebrafish version of the 5-Choice Serial Reaction Time Task (5-
731 CSRTT)[25]. Adult *rbfox1*$^{+/+}$, *rbfox1*$^{+/19del}$ and *rbfox1*$^{19del/19del}$ zebrafish, 7 months old, mixed sexes, were
732 singly housed for a week prior to experiment and remained singly housed for the whole duration of
733 the assay (9 weeks). Fish were tested using the Zantiks AD units. Each unit was provided with a small
734 tank with five apertures and a food hopper insert. The five apertures created five different entry
735 points for the fish, acting like the five nose poke holes of the rodent version of the assay. The food
736 hopper was placed at the opposite side of the five apertures and formed an area for the fish to enter
737 and collect food reward. Below the testing tank there was an integrated screen, used to display
738 white light (stimulus) into the five apertures. Responses were detected when a fish entered these
739 apertures and recorded with an integrated camera placed at the top of the tank. The experiment
740 consisted of five training stages: i) habituation, ii) initiator training, iii) stimulus light training, iv) 5-
741 CSRTT/no delay, v) 5-CSRTT/variable-delay. Details of each stage are provided in Supplementary
742 Table 2.

743 Novel tank diving

744 Novel tank diving is a behavioural test to assess anxiety-like behaviour in adult fish. Response to
745 novel tank was assessed in *rbfox1*$^{+/+}$, *rbfox1*$^{+/19del}$ and *rbfox1*$^{19del/19del}$ 9 months old zebrafish, mixed-
746 sexes, as described previously[33]. Fish were singly housed for a week prior to performing the
747 experiment and acclimatized for at least 1 h in the behavioral room on the testing day. Behavioural
748 assays were conducted between 9 a.m. and 2 p.m. During the test, fish were individually placed into
749 a 1.5 L tank and their behaviour was tracked and recorded using EthoVision system (Noldus). Data
750 were exported in 1 min time bin and analysed as previously described[33]. Experimental groups were
751 randomised during testing. We analyzed three behaviours in response to the novel tank: i) time
752 spent in the bottom of the tank, ii) total distance traveled, and iii) number of transitions to the top–
753 bottom area of the tank.

754 **Whole-body cortisol extraction**

755 Larvae

756 Larval cortisol was extracted from pools of 12 larvae x sample using a modified protocol based on
757 Baiamonte et al. (2016)[35]. Briefly, larvae were snap-frozen upon collection and stored at -20°C until
758 extraction was performed. On the day of extraction, frozen samples were thawed on ice in and
759 homogenised in 400µl of ice-cold 1×PBS for 30 seconds using a Bioruptor (MP Biomedicals). Cortisol
760 was extracted by adding 500µl of ethyl acetate (Sigma) to each homogenate. Samples were
761 vortexed for 30 seconds, centrifuged at 5000rpm for 10 minutes and then snap frozen at −80°C.
762 The organic phase was carefully decanted into glass vials (VWR). The extraction was repeated twice
763 and the combined organic phases were pooled. The pooled ethyl acetate extracts were evaporated
764 at 60°C using a rotary evaporator (IKA). The dried cortisol was resuspended in 200µl of 1xPBS,
765 vortexed for 30 seconds and stored at −20°C until cortisol quantification using a human salivary
766 cortisol ELISA kit (Salimetrics).

767 Adults

768 Adult cortisol was extracted from 4 adult zebrafish whole-body. Fish were weighed and
769 homogenised in 2× volumes (w/v) of 1xPBS using a Bioruptor (MP Biomedicals). Cortisol was
770 extracted using the same ethyl acetate procedure as for larvae. However, after evaporation, to
771 prevent any interference with the assay, residual lipids were eliminated by partitioning the dried
772 extracts between 500µl 1xPBS and 500µl hexane (Sigma). The upper organic layer was discarded and
773 the aqueous phase was retained and stored at −20°C until cortisol quantification using a human
774 salivary cortisol ELISA kit (Salimetrics).

775 **Cortisol measurement**

776 Samples were thawed on ice and 50µl of each was assayed using the Salimetrics human salivary
777 cortisol ELISA kit, following the manufacturer's protocol. Cortisol values for adults were normalised
778 to body weight (ng/g), while larval and juvenile values were normalised to total tissue protein
779 (ng/mg). This assay was validated for use with zebrafish whole-body extracts previously[35,78].
780 Standards, high and low controls and zebrafish samples (25µL) were added to the plate provided
781 with the Salimetric kit, along with Assay Diluent (25µL) for the zero standard. The Enzyme
782 Conjugate was diluted 1:1600 in Assay Diluent and 200µL was dispensed into each well. After
783 mixing for 5minutes at 500rpm, the plate was incubated at RT for 1h and washed four times with
784 1× wash buffer (300µL x well x wash). Next, 200µL of TMB Substrate Solution was added, followed
785 by a 30-minute dark incubation with first 5min mixing. The reaction was stopped with 50µL of Stop
786 Solution, mixed until wells turned yellow, and absorbance was read at 450nm within 10minutes
787 using an OMEGA plate reader (BMG Labtech).

788

789 **Statistical analysis**

790 For qPCR, relative mRNA expressions were calculated using the Pfaffl method[79]. Outliers were
791 identified and removed using Dixon's test ($\alpha = 0.05$)[80]. Differences in gene expression were assessed
792 using a one-way ANOVA followed by Tukey's post-hoc test using GraphPad Software (Prism). For
793 behavioural analysis, all data were analysed with R programming language[75]. Scripts used for
794 analysis are available on GitHub (https://github.com/AdeleLeg). For models where distance moved,
795 distance to zone, velocity, or top halves visits were the response variable, we fitted data to mixed
796 linear models using the "*lme4*" package, and where proportion of responders or proportion of time
797 spent in the bottom third were our response variable, we fitted data to beta regression models using
798 the "*betareg*" package. In all instances, for all experiments, we used genotype as fixed effect, and
799 fish ID and day of experiment as random effects. In the response and habituation to acoustic startle,
800 we used also the stimulus number as fixed effect. As in García-González et al.[33], we reported
801 significant fixed effects as Type II Wald χ^2 from models using the package "*car*," post hoc Tukey's
802 tests were also conducted as necessary with the package "*emmeans*". For the 5-CSRTT, overall
803 correct responses (learning) and anticipatory responses (impulsivity) were assessed using the
804 formulas in Supplementary Table 2. Statistical analysis of mean intensity in *in situ* hybridization
805 images of zebrafish larval sections was performed using ImageJ. Mean intensity values were
806 quantified across specified regions of interest, indicated in Supplementary Figure 5, ensuring that
807 comparable areas of similar dimensions were used for each sample to calculate differences in
808 expression. The resulting values were compared across groups using a paired t-test to determine
809 significant differences using GraphPad Software (Prism). For all experiments, sample size needed to
810 achieve adequate statistical power for detecting a significant effect was determined based on data
811 from previous research or pilot studies. Accepted α level and power were respectively ≤ 0.05 and ≥
812 0.80.

813 **Fertilisation and survival analysis**

814 Fertilisation and survival rates were measured as described previously[19]. For fertilization rate we
815 measured the percentage of fertilized eggs when pairing *rbfox1*$^{19del/19del}$ and compared it with
816 fertilization rate of *rbfox1*$^{+/+}$ siblings. Data were collected upon 3 different mating trials, each trial
817 comprising 3-5 trios (1 male and 2 females). Trials were performed on different weeks, using
818 different trios for each test. Eggs were collected in different Petri dishes, properly labelled to
819 distinguish between trios. Fertilisation rate was determined by averaging across Petri dishes from
820 the same trio and calculated at 6-8hpf. For survival analysis, we measured the percentage of
821 surviving animals (across 3 tanks for each genotype for each batch, to avoid tank effect) from when
822 larvae were added to the nursery (at 5dpf) until 2 months of age, when fish were transferred into
823 adult aquarium.
824

825 **CONTRIBUTIONS**

826 AL conceived the project, designed and conducted the experiments, analysed the data, and wrote
827 the manuscript. JGG designed and performed the CRISPR/Cas9 experiment generating the line. SH,
828 PA, SA, XW and WH contributed to the experiments. NFC and BC edited the manuscript. CHB
829 directed the study, designed the experiments, edited the manuscript, and secured funding. All
830 authors contributed to the article and approved the submitted version.

831 **ACKNOWLEDGMENTS**

832 CHB, AL, SH, PA and WH were supported by the NIH grant U01 DA044400-03. JGG was supported by
833 a 2022 NARSAD Young Investigator Grant (Number #30749) by the Brain & Behavior Research
834 Foundation. NFC and BC were supported by the grants PID2021-127776OB-I100, 202218 31 and
835 2021-SGR-01093 from the Ministry of Science, Innovation and Universities (Spain), Fundació La
836 Marató de TV3, and AGAUR-Generalitat de Catalunya, respectively, and by ICREA Academia 2021.
837 Authors would like to acknowledge SciDraw (https://scidraw.io/) for images used to create the
838 graphical abstract. We thank Prof. Marina Resmini for kindly providing the equipment used to dry
839 cortisol extracts.

840 **CONFLICT OF INTEREST**
841 The authors declare that the research was conducted in the absence of any commercial or financial
842 relationships that could be construed as a potential conflict of interest.
843

844 **REFERENCES**

845 1. Cross-Disorder Group of the Psychiatric Genomics Consortium. Electronic address:
846 plee0@mgh.harvard.edu & Cross-Disorder Group of the Psychiatric Genomics Consortium.
847 Genomic Relationships, Novel Loci, and Pleiotropic Mechanisms across Eight Psychiatric
848 Disorders. *Cell* **179**, 1469-1482.e11 (2019).
849 2. Antón-Galindo, E. *et al.* Pleiotropic contribution of rbfox1 to psychiatric and
850 neurodevelopmental phenotypes in two zebrafish models. *Transl. Psychiatry* **14**, 1–11 (2024).

851 3. Thisse, B. & Thisse, C. ZFIN Publication: Thisse et al., 2004. *ZFIN* http://zfin.org/ZDB-PUB-
852 040907-1.
853 4. Amir-Zilberstein, L. *et al.* Homeodomain Protein Otp and Activity-Dependent Splicing Modulate
854 Neuronal Adaptation to Stress. *Neuron* **73**, 279–291 (2012).
855 5. Abi-Dargham, A. *et al.* Candidate biomarkers in psychiatric disorders: state of the field. *World*
856 *Psychiatry* **22**, 236–262 (2023).
857 6. O'Leary, A. *et al.* Behavioural and functional evidence revealing the role of RBFOX1 variation in
858 multiple psychiatric disorders and traits. *Mol. Psychiatry* **27**, 4464–4473 (2022).
859 7. Lee, J.-A., Tang, Z.-Z. & Black, D. L. An inducible change in Fox-1/A2BP1 splicing modulates the
860 alternative splicing of downstream neuronal target exons. *Genes Dev.* **23**, 2284–2293 (2009).
861 8. Shaughnessy, C. A., Myhre, V. D., Hall, D. J., McCormick, S. D. & Dores, R. M. Hypothalamus-
862 pituitary-interrenal (HPI) axis signaling in Atlantic sturgeon (Acipenser oxyrinchus) and sterlet
863 (Acipenser ruthenus). *Gen. Comp. Endocrinol.* **339**, 114290 (2023).
864 9. Biran, J. *et al.* Splice-specific deficiency of the PTSD-associated gene PAC1 leads to a paradoxical
865 age-dependent stress behavior. *Sci. Rep.* **10**, 9559 (2020).
866 10. Linz, R. *et al.* Acute psychosocial stress increases serum BDNF levels: an antagonistic relation to
867 cortisol but no group differences after mental training. *Neuropsychopharmacology* **44**, 1797–
868 1804 (2019).
869 11. Jeanneteau, F. D. *et al.* BDNF and glucocorticoids regulate corticotrophin-releasing hormone
870 (CRH) homeostasis in the hypothalamus. *Proc. Natl. Acad. Sci. U. S. A.* **109**, 1305–1310 (2012).
871 12. Karatsoreos, I. N. & McEwen, B. S. Psychobiological allostasis: resistance, resilience and
872 vulnerability. *Trends Cogn. Sci.* **15**, 576–584 (2011).
873 13. Miao, Z., Wang, Y. & Sun, Z. The Relationships Between Stress, Mental Disorders, and Epigenetic
874 Regulation of BDNF. *Int. J. Mol. Sci.* **21**, 1375 (2020).

875 14. Suliman, S., Hemmings, S. & Seedat, S. Brain-Derived Neurotrophic Factor (BDNF) protein levels
876 in anxiety disorders: systematic review and meta-regression analysis. *Front. Integr. Neurosci.* **7**,
877 55 (2013).
878 15. Fogel, B. L. *et al.* RBFOX1 regulates both splicing and transcriptional networks in human
879 neuronal development. *Hum. Mol. Genet.* **21**, 4171–4186 (2012).
880 16. Tomassoni-Ardori, F. *et al.* Rbfox1 up-regulation impairs BDNF-dependent hippocampal LTP by
881 dysregulating TrkB isoform expression levels. *eLife* **8**, e49673 (2019).
882 17. Solés-Tarrés, I., Cabezas-Llobet, N., Vaudry, D. & Xifró, X. Protective Effects of Pituitary
883 Adenylate Cyclase-Activating Polypeptide and Vasoactive Intestinal Peptide Against Cognitive
884 Decline in Neurodegenerative Diseases. *Front. Cell. Neurosci.* **14**, (2020).
885 18. Mcewen, B. S. Protection and Damage from Acute and Chronic Stress: Allostasis and Allostatic
886 Overload and Relevance to the Pathophysiology of Psychiatric Disorders. *Ann. N. Y. Acad. Sci.*
887 **1032**, 1–7 (2004).
888 19. Eachus, H. *et al.* Elevated glucocorticoid alters the developmental dynamics of hypothalamic
889 neurogenesis in zebrafish. *Commun. Biol.* **7**, 1–14 (2024).
890 20. Danese, A. & McEwen, B. S. Adverse childhood experiences, allostasis, allostatic load, and age-
891 related disease. *Physiol. Behav.* **106**, 29–39 (2012).
892 21. Bornstein, S. R. *et al.* Stress-inducible-stem cells: a new view on endocrine, metabolic and
893 mental disease? *Mol. Psychiatry* **24**, 2–9 (2019).
894 22. Kinlein, S. A., Wilson, C. D. & Karatsoreos, I. N. Dysregulated Hypothalamic–Pituitary–Adrenal
895 Axis Function Contributes to Altered Endocrine and Neurobehavioral Responses to Acute Stress.
896 *Front. Psychiatry* **6**, (2015).
897 23. Adel, M. R. *et al.* Decreased Brain Serotonin in rbfox1 Mutant Zebrafish and Partial Reversion of
898 Behavioural Alterations by the SSRI Fluoxetine. *Pharmaceuticals* **17**, 254 (2024).

899 24. Lange, M. *et al.* The ADHD-susceptibility gene lphn3.1 modulates dopaminergic neuron
900 formation and locomotor activity during zebrafish development. *Mol. Psychiatry* **17**, 946–954
901 (2012).
902 25. Parker, M. O. *et al.* Development and automation of a test of impulse control in zebrafish. *Front.*
903 *Syst. Neurosci.* **7**, (2013).
904 26. Halberstadt, A. L. & Geyer, M. A. Habituation and sensitization of acoustic startle: opposite
905 influences of dopamine D1 and D2-family receptors. *Neurobiol. Learn. Mem.* **92**, 243–248
906 (2009).
907 27. Burgess, H. A. & Granato, M. Sensorimotor gating in larval zebrafish. *J. Neurosci. Off. J. Soc.*
908 *Neurosci.* **27**, 4984–4994 (2007).
909 28. Cohen, H. *et al.* Blunted HPA axis response to stress influences susceptibility to posttraumatic
910 stress response in rats. *Biol. Psychiatry* **59**, 1208–1218 (2006).
911 29. Leggieri, A. *et al.* Ankk1 Loss of Function Disrupts Dopaminergic Pathways in Zebrafish. *Front.*
912 *Neurosci.* **16**, (2022).
913 30. Zhong, Y. *et al.* RBFOX1 and Working Memory: From Genome to Transcriptome Revealed
914 Posttranscriptional Mechanism Separate From Attention-Deficit/Hyperactivity Disorder. *Biol.*
915 *Psychiatry Glob. Open Sci.* **3**, 1042–1052 (2023).
916 31. Davies, M. N. *et al.* Generalised Anxiety Disorder – A Twin Study of Genetic Architecture,
917 Genome-Wide Association and Differential Gene Expression. *PLOS ONE* **10**, e0134865 (2015).
918 32. Basnet, R. M., Zizioli, D., Taweedet, S., Finazzi, D. & Memo, M. Zebrafish Larvae as a Behavioral
919 Model in Neuropharmacology. *Biomedicines* **7**, E23 (2019).
920 33. García-González, J., de Quadros, B., Havelange, W., Brock, A. J. & Brennan, C. H. Behavioral
921 Effects of Developmental Exposure to JWH-018 in Wild-Type and Disrupted in Schizophrenia 1
922 (disc1) Mutant Zebrafish. *Biomolecules* **11**, 319 (2021).

923 34. Hillman, C., Kearn, J. & Parker, M. O. A unified approach to investigating 4 dpf zebrafish larval
924 behaviour through a standardised light/dark assay. *Prog. Neuropsychopharmacol. Biol.*
925 *Psychiatry* **134**, 111084 (2024).
926 35. Baiamonte, M., Parker, M. O., Vinson, G. P. & Brennan, C. H. Sustained Effects of Developmental
927 Exposure to Ethanol on Zebrafish Anxiety-Like Behaviour. *PLoS ONE* **11**, e0148425 (2016).
928 36. Gene Detail: Allen Brain Atlas: Mouse Brain. https://mouse.brain-map.org/gene/show/92602.
929 37. Brain tissue expression of RBFOX1 - Summary - The Human Protein Atlas.
930 https://www.proteinatlas.org/ENSG00000078328-RBFOX1/brain.
931 38. Thisse, B., Thisse, C. Fast Release Clones: A High Throughput Expression Analysis. (2004)
932 doi:ZDB-PUB-040907-1.
933 39. Grone, B. P. & Maruska, K. P. Divergent evolution of two corticotropin-releasing hormone (CRH)
934 genes in teleost fishes. *Front. Neurosci.* **9**, 365 (2015).
935 40. Sahu, M. P. *et al.* Neurotrophin receptor Ntrk2b function in the maintenance of dopamine and
936 serotonin neurons in zebrafish. *Sci. Rep.* **9**, 2036 (2019).
937 41. Shi, C. *et al.* Hyperandrogenism in POMCa-deficient zebrafish enhances somatic growth without
938 increasing adiposity. *J. Mol. Cell Biol.* **12**, 291–304 (2020).
939 42. Faught, E. & Vijayan, M. M. The mineralocorticoid receptor is essential for stress axis regulation
940 in zebrafish larvae. *Sci. Rep.* **8**, 18081 (2018).
941 43. Tessarollo, L. & Yanpallewar, S. TrkB Truncated Isoform Receptors as Transducers and
942 Determinants of BDNF Functions. *Front. Neurosci.* **16**, (2022).
943 44. Martin, S. C., Marazzi, G., Sandell, J. H. & Heinrich, G. Five Trk Receptors in the Zebrafish. *Dev.*
944 *Biol.* **169**, 745–758 (1995).
945 45. Thisse, C. & Thisse, B. High-resolution in situ hybridization to whole-mount zebrafish embryos.
946 *Nat. Protoc.* **3**, 59–69 (2008).

947 46. Islam, O., Loo, T. X. & Heese, K. Brain-Derived Neurotrophic Factor (BDNF) has Proliferative
948 Effects on Neural Stem Cells through the Truncated TRK-B Receptor, MAP Kinase, AKT, and
949 STAT-3 Signaling Pathways. *Curr. Neurovasc. Res.* **6**, 42–53.
950 47. Finlay, S., Rudd, D., McDermott, B. & Sarnyai, Z. Allostatic load and systemic comorbidities in
951 psychiatric disorders. *Psychoneuroendocrinology* **140**, 105726 (2022).
952 48. Elia, J. *et al.* Rare structural variants found in attention-deficit hyperactivity disorder are
953 preferentially associated with neurodevelopmental genes. *Mol. Psychiatry* **15**, 637–646 (2010).
954 49. van der Kolk, B. Posttraumatic stress disorder and the nature of trauma. *Dialogues Clin.*
955 *Neurosci.* **2**, 7–22 (2000).
956 50. Karin, O. *et al.* A new model for the HPA axis explains dysregulation of stress hormones on the
957 timescale of weeks. *Mol. Syst. Biol.* **16**, (2020).
958 51. Herman, J. P. *et al.* Regulation of the hypothalamic-pituitary-adrenocortical stress response.
959 *Compr. Physiol.* **6**, 603–621 (2016).
960 52. Bale, T. L. & Vale, W. W. CRF and CRF Receptors: Role in Stress Responsivity and Other
961 Behaviors. *Annu. Rev. Pharmacol. Toxicol.* **44**, 525–557 (2004).
962 53. Joëls, M., Karst, H., DeRijk, R. & de Kloet, E. R. The coming out of the brain mineralocorticoid
963 receptor. *Trends Neurosci.* **31**, 1–7 (2008).
964 54. Holsboer, F. The Corticosteroid Receptor Hypothesis of Depression. *Neuropsychopharmacology*
965 **23**, 477–501 (2000).
966 55. Arborelius, L., Owens, M. J., Plotsky, P. M. & Nemeroff, C. B. The role of corticotropin-releasing
967 factor in depression and anxiety disorders. *J. Endocrinol.* **160**, 1–12 (1999).
968 56. Yehuda, R. Status of Glucocorticoid Alterations in Post-traumatic Stress Disorder. *Ann. N. Y.*
969 *Acad. Sci.* **1179**, 56–69 (2009).
970 57. Sheng, J. A. *et al.* The Hypothalamic-Pituitary-Adrenal Axis: Development, Programming Actions
971 of Hormones, and Maternal-Fetal Interactions. *Front. Behav. Neurosci.* **14**, (2021).

972 58. Notaras, M. & van den Buuse, M. Neurobiology of BDNF in fear memory, sensitivity to stress,
973 and stress-related disorders. *Mol. Psychiatry* **25**, 2251–2274 (2020).
974 59. Berton, O. *et al.* Essential Role of BDNF in the Mesolimbic Dopamine Pathway in Social Defeat
975 Stress. *Science* **311**, 864–868 (2006).
976 60. Eckert, A. *et al.* The link between sleep, stress and BDNF. *Eur. Psychiatry* **41**, S282 (2017).
977 61. Nakagomi, A. *et al.* Role of the central nervous system and adipose tissue BDNF/TrkB axes in
978 metabolic regulation. *Npj Aging Mech. Dis.* **1**, 1–11 (2015).
979 62. Fenner, B. M. Truncated TrkB: Beyond a dominant negative receptor. *Cytokine Growth Factor*
980 *Rev.* **23**, 15–24 (2012).
981 63. Cazorla, M. *et al.* Identification of a low–molecular weight TrkB antagonist with anxiolytic and
982 antidepressant activity in mice. *J. Clin. Invest.* **121**, 1846–1857 (2011).
983 64. Azogu, I. & Plamondon, H. Blockade of TrkB receptors in the nucleus accumbens prior to
984 heterotypic stress alters corticotropin-releasing hormone (CRH), vesicular glutamate transporter
985 2 (vGluT2) and glucocorticoid receptor (GR) within the mesolimbic pathway. *Horm. Behav.* **90**,
986 98–112 (2017).
987 65. Bollen, E. *et al.* 7,8-Dihydroxyflavone improves memory consolidation processes in rats and
988 mice. *Behav. Brain Res.* **257**, 8–12 (2013).
989 66. Haapasalo, A., Koponen, E., Hoppe, E., Wong, G. & Castrén, E. Truncated trkB.T1 Is Dominant
990 Negative Inhibitor of trkB.TK+-Mediated Cell Survival. *Biochem. Biophys. Res. Commun.* **280**,
991 1352–1358 (2001).
992 67. Eachus, H., Ryu, S., Placzek, M. & Wood, J. Zebrafish as a model to investigate the CRH axis and
993 interactions with DISC1. *Curr. Opin. Endocr. Metab. Res.* **26**, 100383 (2022).
994 68. Koolhaas, J. M., de Boer, S. F., Coppens, C. M. & Buwalda, B. Neuroendocrinology of coping
995 styles: Towards understanding the biology of individual variation. *Front. Neuroendocrinol.* **31**,
996 307–321 (2010).

997 69. Koolhaas, J. M. *et al.* Coping styles in animals: current status in behavior and stress-physiology.
998 *Neurosci. Biobehav. Rev.* **23**, 925–935 (1999).
999 70. Maussion, G. *et al.* Regulation of a truncated form of tropomyosin-related kinase B (TrkB) by
1000 Hsa-miR-185* in frontal cortex of suicide completers. *PloS One* **7**, e39301 (2012).
1001 71. Keatinge, M. *et al.* CRISPR gRNA phenotypic screening in zebrafish reveals pro-regenerative
1002 genes in spinal cord injury. *PLOS Genet.* **17**, e1009515 (2021).
1003 72. Dobrzycki, T., Krecsmarik, M. & Monteiro, R. Genotyping and Quantification of In Situ
1004 Hybridization Staining in Zebrafish. *JoVE J. Vis. Exp.* e59956 (2020) doi:10.3791/59956.
1005 73. Schindelin, J. *et al.* Fiji: an open-source platform for biological-image analysis. *Nat. Methods* **9**,
1006 676–682 (2012).
1007 74. Wullimann, M. F., Rupp, B. & Reichert, H. The brain of the zebrafish Danio rerio: a
1008 neuroanatomical atlas. in *Neuroanatomy of the Zebrafish Brain: A Topological Atlas* (eds.
1009 Wullimann, M. F., Rupp, B. & Reichert, H.) 19–87 (Birkhäuser, Basel, 1996). doi:10.1007/978-3-
1010 0348-8979-7_5.
1011 75. R Development Core Team. R: A language and environment for statistical computing.
1012 https://stat.ethz.ch/pipermail/r-help/2008-May/161481.html (2008).
1013 76. Gutiérrez, H. C. *et al.* Screening for drugs to reduce zebrafish aggression identifies caffeine and
1014 sildenafil. *Eur. Neuropsychopharmacol.* **30**, 17–29 (2020).
1015 77. Parker, M. O., Brock, A. J., Sudwarts, A. & Brennan, C. H. Atomoxetine reduces anticipatory
1016 responding in a 5-choice serial reaction time task for adult zebrafish. *Psychopharmacology*
1017 *(Berl.)* **231**, 2671–2679 (2014).
1018 78. Alderman, S. L. & Bernier, N. J. Ontogeny of the corticotropin-releasing factor system in
1019 zebrafish. *Gen. Comp. Endocrinol.* **164**, 61–69 (2009).
1020 79. Pfaffl, M. W. A new mathematical model for relative quantification in real-time RT–PCR. *Nucleic*
1021 *Acids Res.* **29**, e45 (2001).

80. Dean, R. B. & Dixon, W. J. Simplified Statistics for Small Numbers of Observations. *Anal. Chem.* **23**, 636–638 (1951).

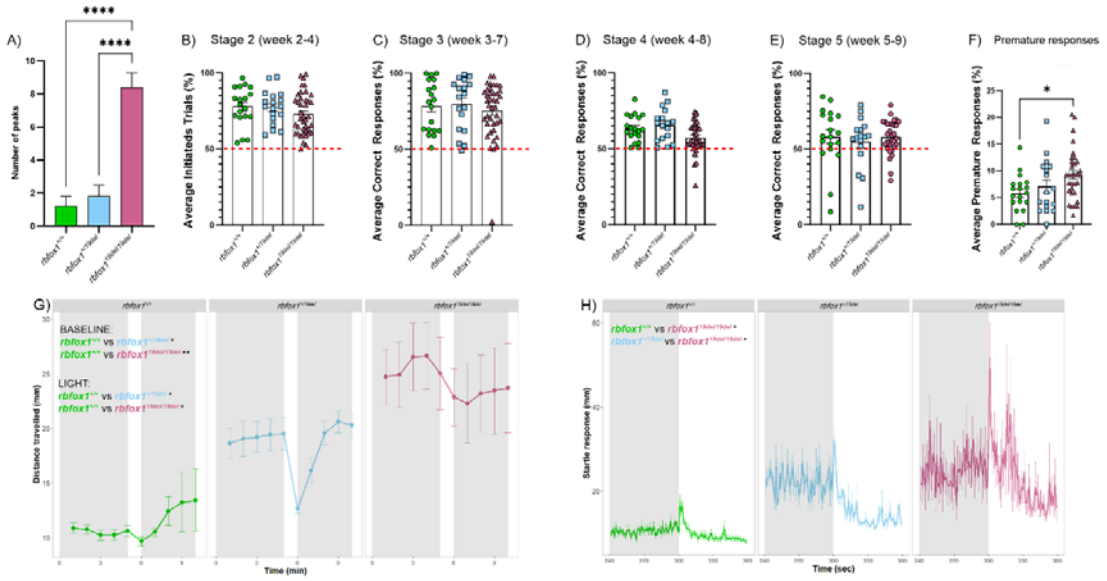

Figure 1. *rbfox1* mutant fish show hyperactivity, impulsivity and hyperarousal behaviour. A number of peaks/swimming burst (acceleration events when the fish travelled > 5 mm in < 12 s); N = *rbfox1*$^{+/+}$ 24; *rbfox1*$^{+/19del}$ 24; *rbfox1*$^{19del/19del}$ 24. **B-F)** 5-choice serial reaction time task in adult (7 months old) zebrafish (*rbfox1*$^{+/+}$, *rbfox1*$^{+/19del}$, *rbfox1*$^{19del/19del}$): **B)** number of initiated trials during stage 2 (weeks 2-4); all *rbfox1*$^{+/+}$ (19), all *rbfox1*$^{+/19del}$ (18) and all *rbfox1*$^{19del/19del}$ (40) moved to the next stage; **C-E)** average correct responses for stages 3-5 (weeks 3-9); **C)** at the end of stage 3 (weeks 3-7), all *rbfox1*$^{+/+}$ (19), 17 *rbfox1*$^{+/19del}$ and 39 *rbfox1*$^{19del/19del}$ moved to the next stage; **D)** at the end of stage 4 (weeks 4-8), all *rbfox1*$^{+/+}$ (19), all *rbfox1*$^{+/19del}$ (17) and 33 *rbfox1*$^{19del/19del}$ moved to the next

stage; **E)** at the end of stage 5 (weeks 5-9), 15 *rbfox1*$^{+/+}$, 13 *rbfox1*$^{+/19del}$ and all *rbfox1*$^{19del/19del}$ (33) showed ≥ 50% correct responses; **F)** premature responses during stage 5 (weeks 5-9). Each dot, square or triangle in D-H) represents a single adult zebrafish *rbfox1*$^{+/+}$, *rbfox1*$^{+/19del}$ and *rbfox1*$^{19del/19del}$ respectively; N = *rbfox1*$^{+/+}$ 19; *rbfox1*$^{+/19del}$ 18; *rbfox1*$^{19del/19del}$ 40. **G-H)** Forced light-dark transition assay in 5dpf zebrafish larvae (*rbfox1*$^{+/+}$, *rbfox1*$^{+/19del}$, *rbfox1*$^{19del/19del}$): **G)** distance travelled during the 10 min assay; **H)** 1 sec time bin resolution plots of the dark-light transition; N = *rbfox1*$^{+/+}$ 43; *rbfox1*$^{+/19del}$ 34; *rbfox1*$^{19del/19del}$ 37. All larvae employed in behavioural experiments were progeny of *rbfox1*$^{+/19del}$ in-cross and were genotyped after experiments and prior to data analysis. In all graphs: bars represent standard error of the mean (SEM); * $p < 0.05$; ** $p < 0.01$; *** $p < 0.001$; **** $p < 0.0001$.

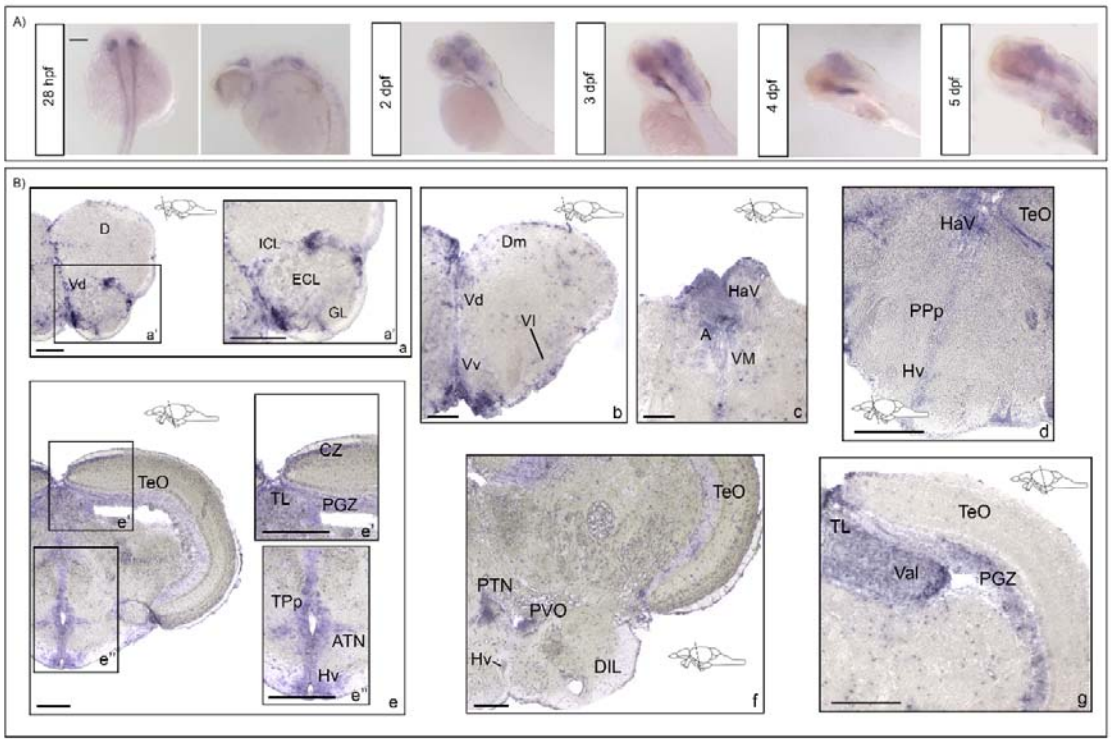

Figure 2. *rbfox1* is expressed in regions of the brain associated with stress response, social and emotional behaviour, reward and learning. A) *rbfox1* whole mount *in situ* hybridization (ISH) on zebrafish larvae at 28 hours post fertilization and 3-4-5 days post fertilization. **B)** *rbfox1* ISH on adult zebrafish (a - d) forebrain and (e-g) mid-/hind-brain transverse sections. Black boxes represent the region of the brain showed in higher magnification panels. Schematic depictions of the lateral view of the zebrafish brain indicate position of levels illustrated by ISH. Scale bars: 200 µm in A), 100 µm in B) a-c, e, f); 50 µm in B) a', d, e', e'', g. Abbreviations: A, anterior tuberal nucleus; ATN, anterior thalamic nucleus; CZ, central zone of the TeO; D, dorsal area of dorsal telencephalon; DIL, diffuse nucleus of the inferior lobe of the hypothalamus; Dm, dorsal area of medial telencephalon; ECL, external cellular layer; GL, glomerular layer; HaV, ventral area of the habenula; Hv, ventral hypothalamus; ICL, internal cellular layer; PGZ, periventricular gray zone; PPp, parvocellular preoptic nucleus, posterior part; PTN, posterior tuberal nucleus of the hypothalamus; PVO, paraventricular organ; TeO, optic tectum; TL, longitudinal tori; TPp, periventricular nucleus of the posterior tuberculum; Val, valvula cerebelli; Vd, ventral area of dorsal telencephalon; Vl, central area of lateral telencephalon; VM, ventromedial nucleus; Vv, ventral area of ventral telencephalon.

1070

1071

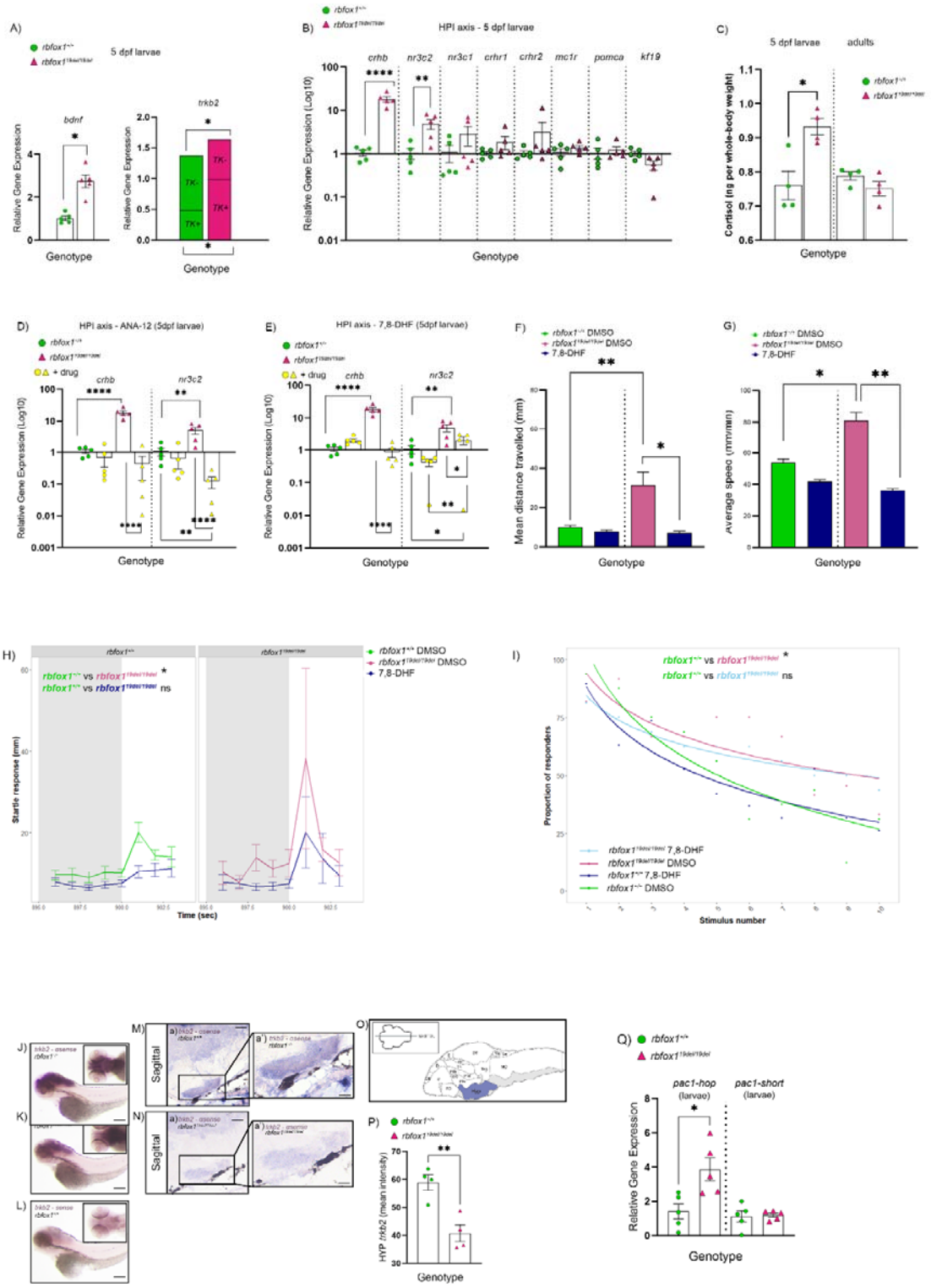

1072

1073 **Figure 3. *rbfox1* LoF disrupts zebrafish larvae HPI axis, *bdnf/trkb2* pathway and *pac1a***

1074 **expression**. **TRKB modulation restore HPI gene expression and behaviour. A)** Expression levels of
1075 *bdnf* and *trkb2* full-length (*TK+*) *and* truncated (*TK-*) in 5 days post fertilisation (dpf) larvae (*rbfox1*$^{+/+}$
1076 and *rbfox1*$^{19del/19del}$). *trkb2* expression is shown in a stacked bar format, where the directly measured
1077 *TK+* (long form) is shown as the lower portion and the inferred *TK-* (short form) is shown on top. **B)**
1078 Expression levels of HPI axis genes *crhb*, *nr3c2*, *nr3c1, crhr1, crhr2, mc1r, pomca* and *kf19* in 5dpf
1079 larvae (*rbfox1*$^{+/+}$ and *rbfox1*$^{19del/19del}$). **C)** Whole-body cortisol measurement of 5dpf larvae (left panel)
1080 and adult fish (right panel) in resting physiological conditions. Cortisol values are normalised per
1081 whole-body homogenate (g) (*rbfox1*$^{+/+}$ and *rbfox1*$^{19del/19del}$). **D-E)** Expression levels of *crhb* and *nr3c2*
1082 in presence or absence of the TRKB selective **D)** antagonist ANA-12 and **E)** agonist 7,8-DHF in 5dpf
1083 larvae (*rbfox1*$^{+/+}$ and *rbfox1*$^{19del/19del}$). **F-I)** Behavioural assays in presence and absence of the TRKB
1084 agonist 7,8-DHF in *rbfox1* larvae (*rbfox1*$^{+/+}$ and *rbfox1*$^{19del/19del}$): **F)** mean distance travelled, **G)**
1085 average speed, **H)** startle response to white light stimulus and **I)** Proportion of responders over time
1086 in the response and habituation to acoustic startle assay. **J-N)** Whole mount *in situ* hybridisation
1087 (ISH) for *trkb2* anti-sense riboprobe in **J)** *rbfox1*$^{+/+}$ and **K)** *rbfox1*$^{19del/19del}$ and **L)** *trkb2* sense riboprobe
1088 in *rbfox1*$^{+/+}$ 5dpf larvae (lateral view in the main boxes and dorsal view in the smaller boxes on the
1089 top right corner). **M, N)** Sagittal cryosection of *trkb2* ISH in **M)** *rbfox1*$^{+/+}$ and **N)** *rbfox1*$^{19del/19del}$ 5 dpf
1090 larvae. Black boxes in **M-a)** and **N-a)** represent the region of the brain showed in higher
1091 magnification panels in **M-a')** and **N-a')**. Scale bars: 200 µm in J), K) and L); 100 µm in M-a) and N-a);
1092 50 µm in M-a') and N-a'). **O)** Schematic depiction (sagittal) of zebrafish larval brain indicating
1093 position of levels illustrated by ISH on sagittal cryosections. **P)** *trkb2* ISH intensity mean in the
1094 hypothalamus of 5dpf zebrafish larvae, *rbfox1*$^{+/+}$ versus *rbfox1*$^{19del/19del}$. N = 4 larvae x genotype. **Q)**
1095 Expression levels of *pac1-hop* and *pac1-short* in *rbfox1*$^{+/+}$ and *rbfox1*$^{19del/19del}$ 5 dpf larvae. For qPCR
1096 experiments, reference genes were actin – β 2 (*actb2*) and ribosomal protein L13a (*rpl13a*). Each
1097 green dot/pink triangle in A-D, K-L) represents a pool of 15 larval heads (eyes and jaw removed),
1098 while yellow ones represent larvae exposed to TRKB drugs. Where indicated, we used Log_{10}
1099 transformation to normalize the data facilitating a clearer visualisation of trends within the dataset.
1100 All larvae employed were progeny of *rbfox1*$^{+/19del}$ in-cross and were genotyped after experiments and
1101 prior to data analysis. For cortisol measurement (G), each dot/triangle represent a pool of 12 larvae
1102 in the left panel (larvae) and a single whole zebrafish in the right panel (adult fish). In all graphs: bars
1103 represent standard error of the mean (SEM); * $p < 0.05$; ** $p < 0.01$; **** $p < 0.0001$.

1104

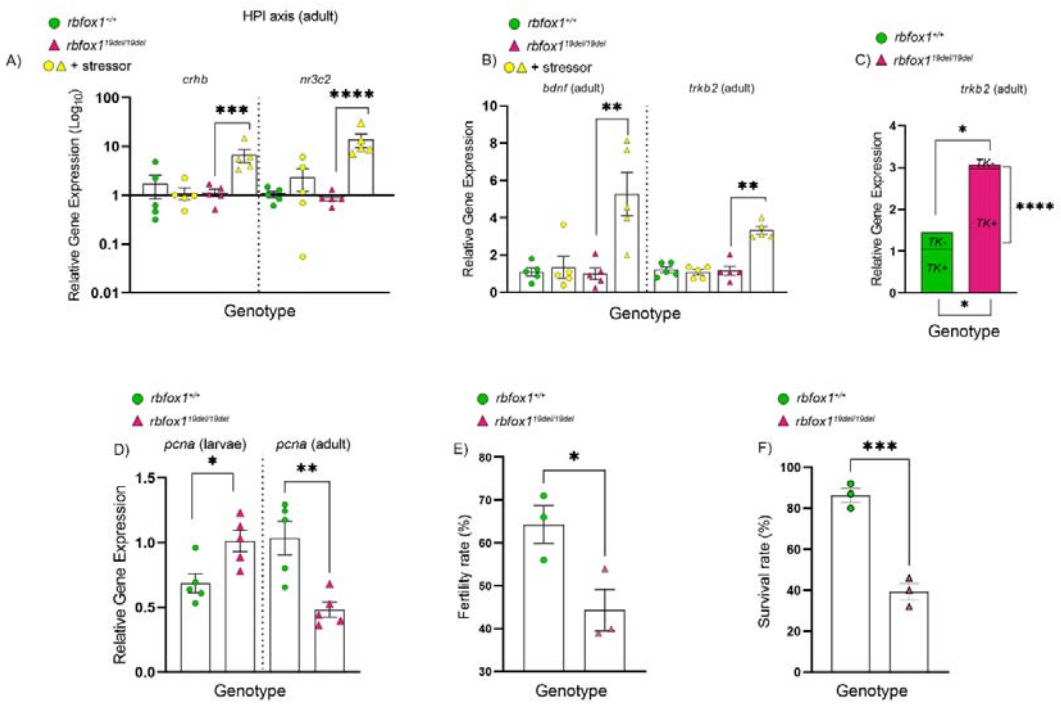

Figure 4. *rbfox1* mutants undergo adaptive mechanisms and allostatic overload during development. Expression levels of **A)** HPI axis genes corticotropin releasing hormone b (*crhb*), mineral corticoid receptor (*mr*) and glucocorticoid receptor (*gr*) and of **B)** *bdnf* and *trkb2* truncated/full-length (*TK-/TK+*) (common primers) in adult zebrafish brain (*rbfox1*$^{+/+}$ and *rbfox1*$^{19del/19del}$) in normal resting conditions and after exposure to a stressor (novel tank diving). **C)** Expression levels of the *trkb2 TK+* and *TK-* in adult zebrafish brain (*rbfox1*$^{+/+}$ and *rbfox1*$^{19del/19del}$) after exposure to a stressor.). *trkb2* expression is shown in a stacked bar format, where the directly measured *TK+* (long form) is shown as the lower portion and the inferred *TK-* (short form) is shown on top. **D)** Expression levels of proliferating cell nuclear antigen (*pcna*) in 5 days post fertilisation zebrafish larvae and adult zebrafish brain (*rbfox1*$^{+/+}$ and *rbfox1*$^{19del/19del}$) in normal resting conditions. **E)** Fertility rate and **F)** survival rate of *rbfox1*$^{+/+}$ and *rbfox1*$^{19del/19del}$. Each green dot/pink triangle in A-B) represents a single adult *rbfox1*$^{+/+}$ or *rbfox1*$^{19del/19del}$ brain under resting physiological conditions respectively, while yellow dots/triangles represent *rbfox1*$^{+/+}$ or *rbfox1*$^{19del/19del}$ brain after stress exposure respectively. In B) each green dot/pink triangle represents single adult *rbfox1*$^{+/+}$ or *rbfox1*$^{19del/19del}$ brain after stress exposure respectively. In D) for larvae each green dot/pink triangle represents a pool of *rbfox1*$^{+/+}$ or *rbfox1*$^{19del/19del}$ 15 larval heads (eyes and jaw removed) respectively; for adults each green dot/pink triangle represents a single adult *rbfox1*$^{+/+}$ or *rbfox1*$^{19del/19del}$ brain respectively. In E) each dot/triangle represents average fertility of 3-5 trios (1 male and 2 females) assessed over 2-3 petri dish (50 embryos per dish) per trio. Each trio belonged to a different tank (for each genotype for each batch) to avoid tank effect). In F) each dot/triangle represents the percentage of survival of a single fish stock comprising 50 larvae. For qPCR experiments, reference genes were actin – β 2 (*actb2*) and ribosomal protein L13a (*rpl13a*). Where indicated, we used Log_{10} transformation to normalize the data facilitating a clearer visualization of trends within the dataset. All larvae employed were progeny of *rbfox1*$^{+/19del}$ in-cross and were genotyped after experiments and prior to data analysis. In all graphs: bars represent standard error of the mean (SEM); * $p < 0.05$; ** $p < 0.01$; *** $p < 0.001$; **** $p < 0.0001$.

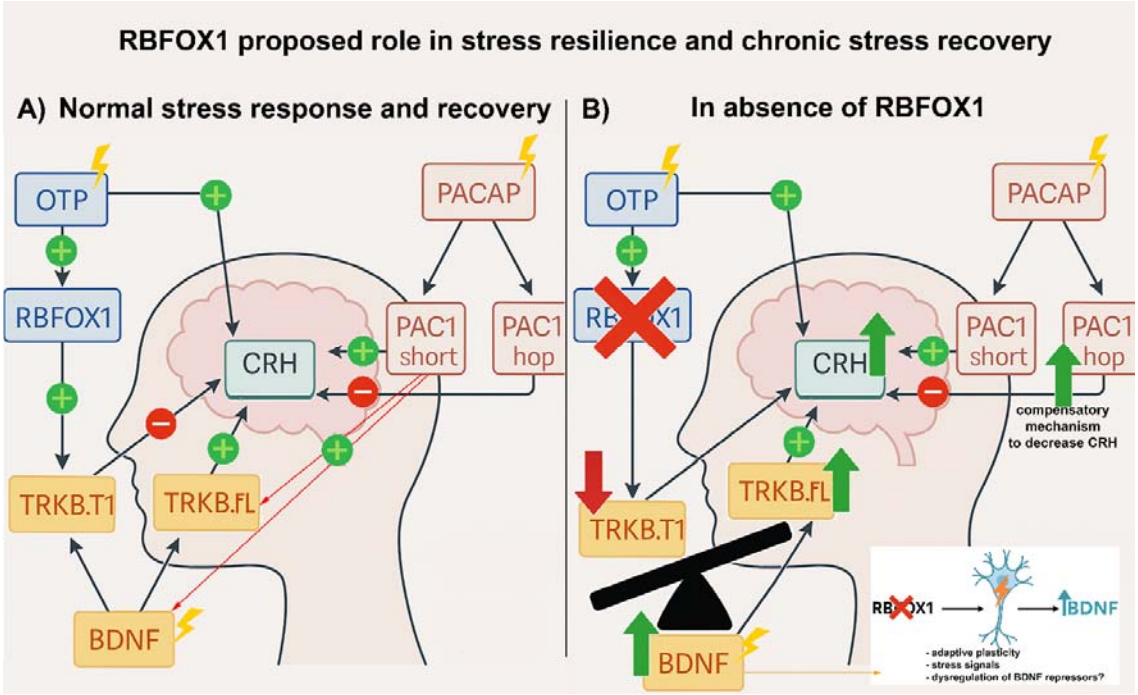

Figure 5. RBFOX1 role in stress resilience and chronic stress recovery: proposed mechanism of action. A) In response to stressful challenges (yellow flash), BDNF expression levels increase, stimulating *CRH* transcription via TRKB.FL/TK+ (yellow pathway). At the same time, stress triggers also *PACAP* transcription (red pathway) and OTP-mediated transcription of *RBFOX1* and *CRH* (blue pathway). PACAP stimulates *CRH* transcription via PAC1-short and inhibits *CRH* transcription via PAC1-hop. PACAP binding to PAC1-short also increases *BDNF* transcription (red line) and enhances TRKB.FL/TK+ activity (red line). RBFOX1 functions as a "switch" maintaining the balance between full-length/truncated TRKB isoforms (promoting TRKB mRNA stability and/or alternative splicing): during the stress recovery phase, *RBFOX1* switches the balances in support of *TRKB.T1/TK-* isoform, decreasing *CRH* levels and turning off the HPA axis. **B)** *RBFOX1* deletion leads to an increase in *BDNF* expression levels (yellow arrow and white box) and an unbalance between *TRKB.FL/TK+* (increased) and *TRKB.T1/TK-* (decreased) isoforms. Such dysregulation ultimately leads to an increase in *CRH* transcription (and possible hyperactivation of the HPA axis), and increase in PAC1-hop levels as possible compensatory mechanism. Our data suggest that RBFOX1-mediated regulation of *TRKB.T1/TK-* mRNA stability and/or alternative splicing is necessary to promote neuroplasticity and stress resilience.

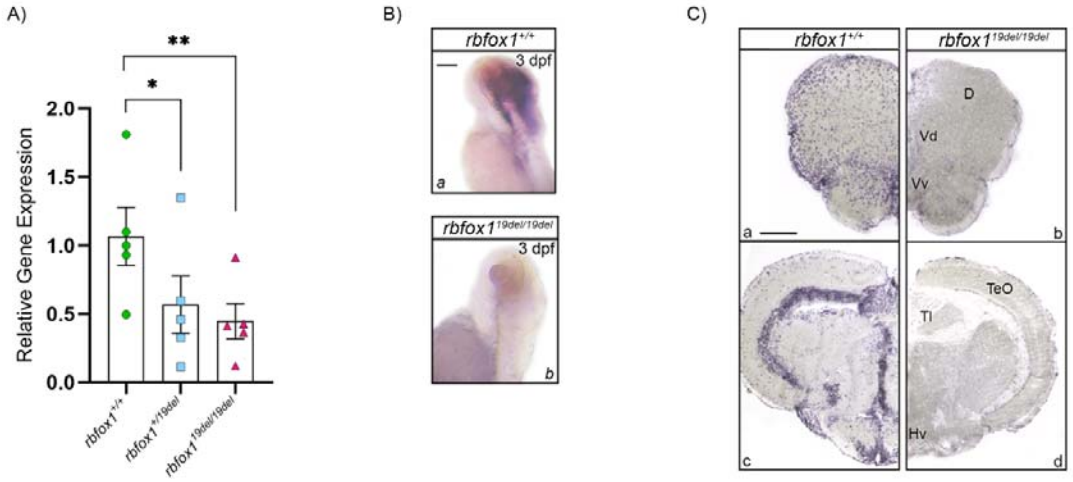

Supplementary Figure 1. Generation of a *rbfox1* loss of function line. A) *rbfox1* mRNA expression in *rbfox1*$^{+/+}$, *rbfox1*$^{+/19del}$ and *rbfox1*$^{19del/19del}$ 5 days post fertilisation (dpf) larvae. *In situ* hybridisation on **B)** whole mount zebrafish larvae at 3dpf, a) *rbfox1*$^{+/+}$ and b) *rbfox1*$^{19del/19del}$ and **C)** adult transverse sections of *rbfox1*$^{+/+}$ (a) fore- and (c) mid- brain and *rbfox1*$^{19del/19del}$ (b) fore- and (d) mid-brain. In A) each dot/square/triangle represents a pool of *rbfox1*$^{+/+}$ or *rbfox1*$^{19del/19del}$ 15 larval heads (eyes and jaw removed) respectively. For qPCR experiments, reference genes were actin – β 2 (*actb2*) and ribosomal protein L13a (*rpl13a*). All larvae employed were progeny of *rbfox1*$^{+/19del}$ in-cross and were genotyped after experiments and prior to data analysis. In A): bars represent standard error of the mean (SEM); * $p < 0.05$; ** $p < 0.01$. Scale bars: 200 µm in B); 100 µm in C). Abbreviations: D, dorsal area of dorsal telencephalon; Hv, ventral hypothalamus; TeO, optic tectum; Tl, longitudinal tori; Vd, ventral area of dorsal telencephalon; Vv, ventral area of ventral telencephalon. N = 4 x genotype.

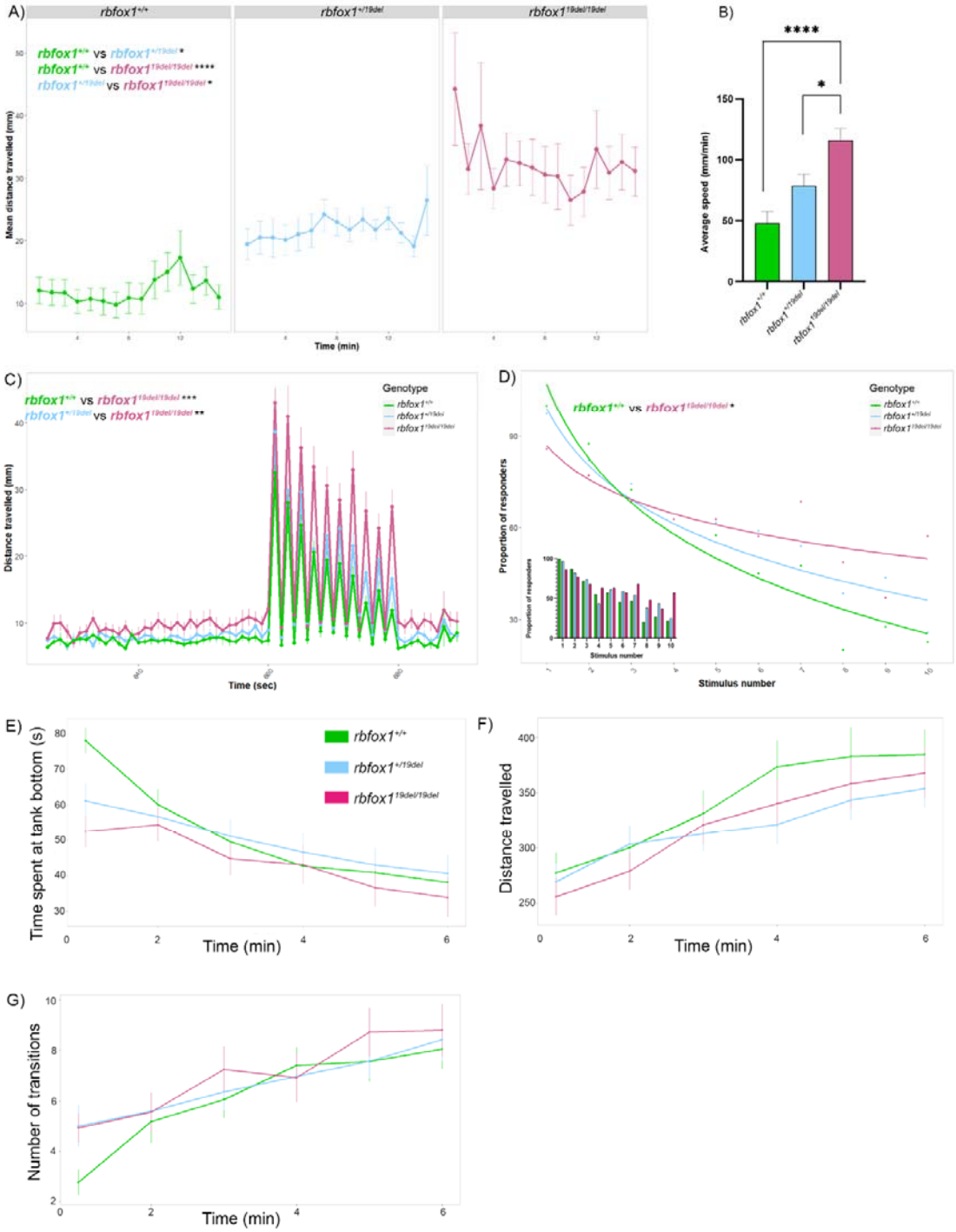

Supplementary Figure 2. *rbfox1* mutant fish show hyperactivity, impulsivity and hyperarousal behaviour. A-B) Locomotion assay in 5 days post fertilization (dpf) zebrafish larvae (*rbfox1*$^{+/+}$, *rbfox1*$^{+/19del}$, *rbfox1*$^{19del/19del}$): **A)** distance travelled during 15 min; **B)** average speed; N (A-B) = *rbfox1*$^{+/+}$ 24; *rbfox1*$^{+/19del}$ 24; *rbfox1*$^{19del/19del}$ 24. 5-9). **C-D)** Response and habituation to acoustic startle assay in 5dpf zebrafish larvae (*rbfox1*$^{+/+}$, *rbfox1*$^{+/19del}$, *rbfox1*$^{19del/19del}$): **C)** mean distance travelled during the assay; **D)** rate of habituation over time/stimuli; N = *rbfox1*$^{+/+}$ 40; *rbfox1*$^{+/19del}$ 39; *rbfox1*$^{19del/19del}$ 35. E-G) Novel tank diving assay in *rbfox1*$^{+/+}$, *rbfox1*$^{+/19del}$ *and rbfox1*$^{19del/19del}$. **E)** Time spent at the bottom of the tank. **F)** Distance travelled during the assay and **G)** number of transitions

between the top and bottom of the tank. N = *rbfox1*$^{+/+}$, 50; *rbfox1*$^{+/19del}$ 54; *rbfox1*$^{19del/19del}$ 54. Bars represent standar error of the mean (SEM). All larvae employed in behavioural experiments were progeny of *rbfox1*$^{+/19del}$ in-cross and were genotyped after experiments and prior to data analysis. In all graphs: bars represent standard error of the mean (SEM); * $p < 0.05$; ** $p < 0.01$; *** $p < 0.001$; **** $p < 0.0001$.

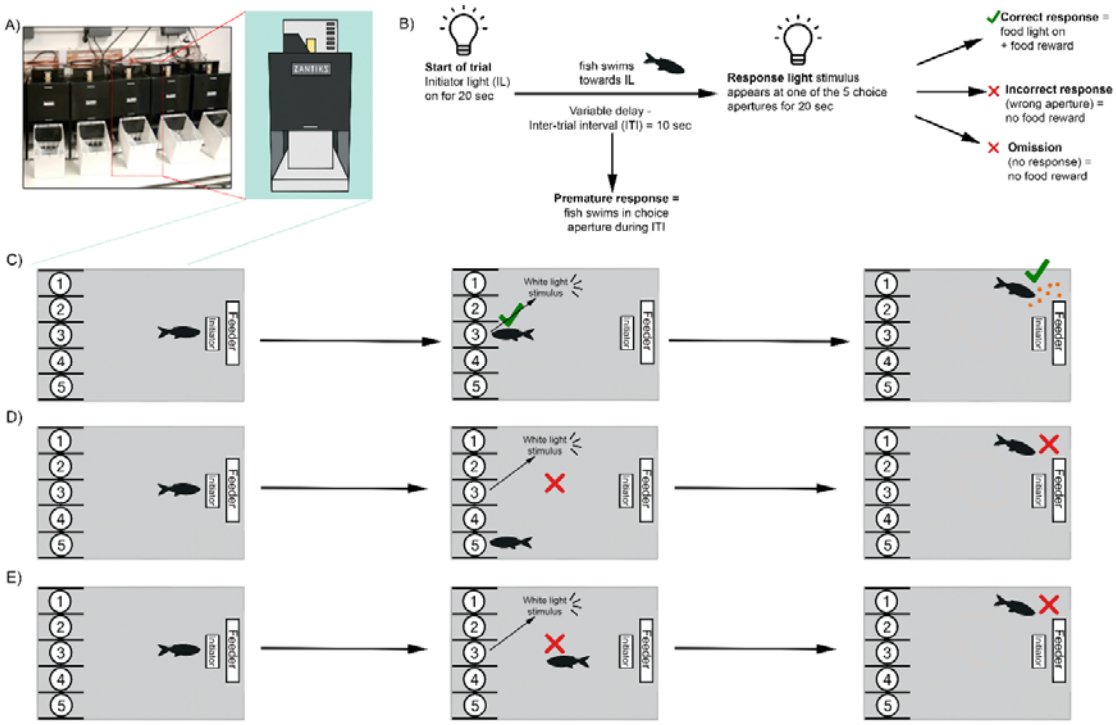

Supplementary Figure 3. 5-choice serial reaction time task. A) Zantiks behavioural testing apparatus used in the laboratory (left panel) and a schematic representation of a single Zantiks chamber (right panel). **B)** Schematic overview of the pipeline in a single 5-choice trial, including initiation, stimulus presentation and response outcome. **C-E)** Illustrative diagrams of representative trial outcomes as depicted in the pipeline in panel B), including C) correct response, D) incorrect response and E) omission.

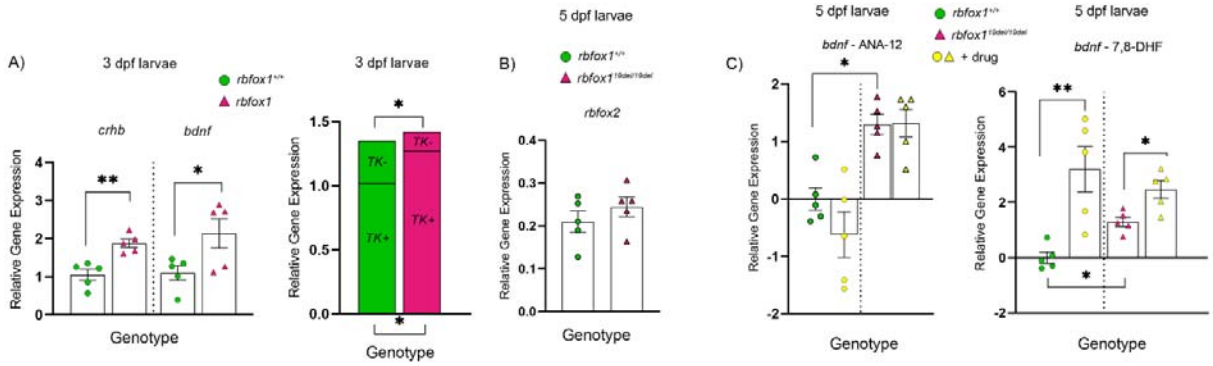

Supplementary Figure 4. A) *crhb* and *bdnf* (left) and trkb2 short and long isoform (right) expression levels in 3 days old larvae, *rbfox1*$^{+/+}$ and *rbfox1*$^{19del/19del}$. **B)** *rbfox2* expression levels in 5 days old larvae, *rbfox1*$^{+/+}$ and *rbfox1*$^{19del/19del}$. **C)** *bdnf* expression levels in 5 days old larvae, *rbfox1*$^{+/+}$ and *rbfox1*$^{19del/19del}$, following chronic exposure to either ANA-12 (left) or 7,8-DHF (right). Actin – β 2 (*actb2*) and ribosomal protein L13a (*rpl13a*) were used as reference genes. Dots/triangles represent pool of 15 larval heads (eyes and jaw removed). Bars represent standard error of the mean (SEM). N = *rbfox1*$^{+/+}$ 5; *rbfox1*$^{19del/19del}$ 5.

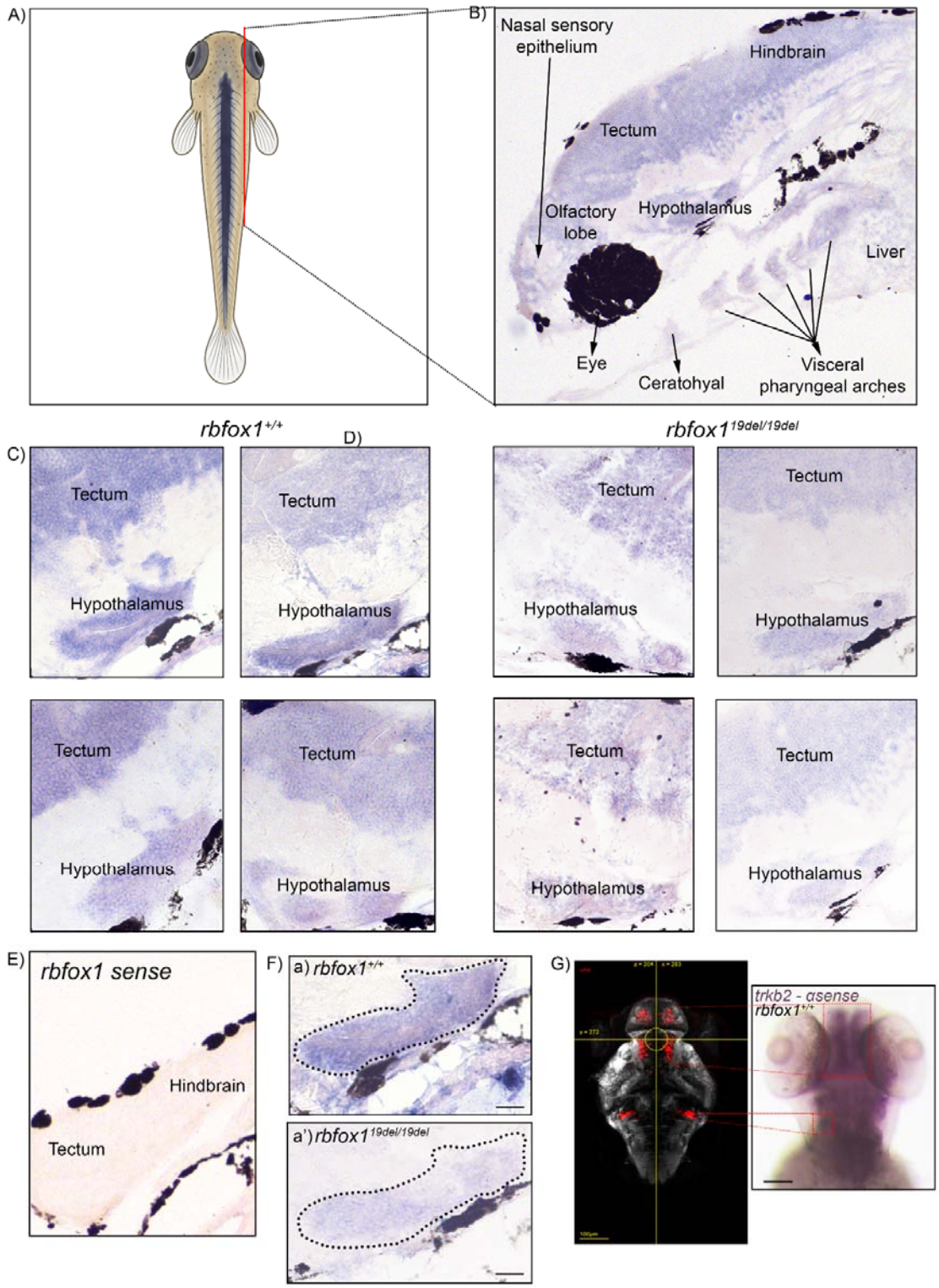

1205

1206 **Supplementary Figure 5.** Details of *in situ* hybridisation experiments for *trkb2* anti-sense riboprobe
1207 on 5 days post fertilisation zebrafish larvae, sagittal sections. **A)** Schematic representation indicating
1208 the level of the anatomical section (red line). **B)** Representative sagittal section of zebrafish larva
1209 stained for *rbfox1* (anti-sense riboprobe), with anatomical regions labelled in black according to ZFIN
1210 atlas of zebrafish larvae (https://zfin.org/zf_info/anatomy.html). **C-D)** Overview of zebrafish larvae

hypothalamus (sagittal sections), *rbfox1*$^{+/+}$ (four panels on the left) and *rbfox1*$^{19del/19del}$ (four panels on the right). Each panel corresponds to a different animal. N = 4 per genotype. Sections have been placed on the same slide and were stained under the same conditions. **E)** *In situ* hybridisation for *trkb2* sense riboprobe on 5 days post fertilisation zebrafish larva, sagittal section. **F)** Example of areas selected (areas enclosed by the black dotted lines) to calculate *trkb2* mean intensity in the hypothalamus of a) zebrafish *rbfox1*$^{+/+}$ (left panel) and a') *rbfox1*$^{19del/19del}$ (right panel) larval sections. **G)** Comparison of *trkb2* and crhb expression in the larval zebrafish brain. The left panel displays crhb-expressing cells in the larval brain from the publicly available MapZebrain atlas (https://mapzebrain.org/atlas/2d). The right panel shows whole-mount *in situ* hybridisation for *trkb2* expression in 5 days old zebrafish larva. Scale bars: F) 50 µm; G) 100 µm.

Supplementary Table 1. List of primers used for qPCR experiments.

Gene (purpose)	Gene acronym	Accession number	Sequence (5' to 3')	Product size (bp)
actin, β 2 (housekeeping)	*actb2*	NM_181601.5	Forward: CGAGCTGTCTTCCCATCCA	86
			Reverse: TCACCAACGTAGCTGTCTTTCTG	
ribosomal protein L13a (housekeeping)	*rpl13a*	NM_212784.1	Forward: TCTGGAGGACTGTAAGAGGTATGC	148
			Reverse: AGACGCACAATCTTGAGAGCAG	
RNA binding fox-1 homolog 1	*rbfox1**	NM_001005596.1	Forward: AACAGCATACAGGCGGTCTC	110
			Reverse: GGCTGCGTTTTGATTTCTGT	
corticotropin releasing hormone	*crhb*	NM_001007379.1	Forward: CGAGACATCCCAGTATCCAAAAAG	60
			Reverse: TCCAACAGACGCTGCGTTAA	
mineralcorticoid receptor	*nr3c2*	NM_001100403	Forward: CTTCCAGGTTTCCGCAGTCTAC	75
			Reverse: GGAGGAGAGACACATCCAGGAAT	
glucocorticoid	*nr3c1*	NM_001020711	Forward:	90

receptor		.3	ACTCCATGCACGACTTGGTG Reverse: GCATTTCGGGAAACTCCACG	
brain derived neurotrophic factor	*bdnf*	XM_009303234.3	Forward: AGCAGACTGTCTTTTGTTGTGTT Reverse: CTTAAGCTCACACAGGTGCC	123
neurotrophic tyrosine kinase, receptor, type 2b (common primers)	*trkb2.TK+/TK-*	NM_001197161.2	Forward: CGCATACCTGACGTGGATCA Reverse: AAGCAACCCCAGCTATTCCC	130
neurotrophic tyrosine kinase, receptor, type 2b (tyrosine kinase domain primers)	*trkb2.TK+*	NM_001197161.2	Forward: TGAAAGTGGGCGAGCAGATT Reverse: CATCTGGACCATGAGCCCTG	173
adenylate cyclase activating polypeptide 1a (pituitary) receptor type I (adcyap1r1a) transcript variants 1 and 2	*pac1a-hop*	NM_001142926.1 NM_001013444.2	Forward: CAGAAATGCTTCAGTGAGCCC Reverse: CCAGACGTAGCGTGATGGTA	82
adenylate cyclase activating polypeptide 1a (pituitary) receptor type I (adcyap1r1a), transcript variant 3	*pac1a-short*	NM_001142925.1	Forward: GATTCTGGCTGCTGGGACAT Reverse: GCGCGCCAGACGTAGATAAA	183
RNA binding fox-1 homolog 2	*rbfox2*	NM_214746.2	Forward: CCGTATGCTAACGGGGACAG Reverse: ACCCTGGAACTGCGTAGAAC	106
corticotropin releasing hormone receptor 1	*crhr1*	XM_691254.7	Forward: TCGGTGTTGAGTCTCATGCC Reverse: CGCGTGCGGGTAAAATGTAG	186
corticotropin releasing hormone receptor 2	*crhr2*	NM_001113644.1	Forward: CTGACGAGCCACCTGTTTCT Reverse: TTACCCGTCCACCGATCAAC	207
melanocortin	*mc1r*	NM_180970.1	Forward: TGCTGGTCACCGCAAAAATG	115

receptor			Reverse: ATATAACGGTCCGCCGCAAT	
propiomelanocortin a	*pomca*	NM_181438.3	Forward: CTGCCATAGATGATGCCGGT	140
			Reverse: TGCGTTTGCTCGTCTCTGAT	
Krüppel-like factor 9	*klf9*	NM_001128729.1	Forward: GACAAACTAACCGGCGAGGA	153
			Reverse: GTTCTCCCGATTCTCCGCAT	

1232 * These primers amplify all *Danio rerio rbfox1* isoforms available on NCBI: XM_068216713.1,
1233 XM_068216714.1, XM_017354041.3, XM_068216717.1, XM_068216718.1, XM_017354043.3,
1234 XM_017354044.3, XM_068216722.1, XM_017354045.3, XM_068216724.1, XM_068216725.1,
1235 XM_068216726.1, XM_068216728.1, XM_017354049.3 XM_068216731.1.
1236
1237
1238 **Supplementary Table 2.** 5-Choice Serial Reaction Time Task stages (5-CSRTT) and corresponding
1239 descriptions. Source: https://zantiks.com
1240

Stage	Name of the stage	Description
Stage 1	Habituation	All lights are illuminated (initiator light, five choice lights and food light) for 20 sec and the food is released. All fish are moved to the next stage of training after 1 week.
Stage 2	Initiator training	Initiator light is on for 20 sec. If the fish swims to the illuminated initiation area, an initiated trial is recorded and the feeder releases food with the food light on for 20 sec. This is followed by 10 sec ITI. The initiator training is repeated for 30 trials. Fish move to the next stage when the average of initiated trials to total trials over five days is > 50%.
Stage 3	Stimulus light training	The initiation light is on for 20 sec. If the fish swims to the illuminated initiation area, an initiated trial is recorded and all five choice lights are illuminated for 20 sec. If the fish swims to any illuminated choice area whilst the light is on, a correct response is recorded and the feeder releases food with the food light on for 20 sec. This is followed by 10 sec ITI. The stimulus light training is repeated for 30 trials. Fish move to the next stage when both the average of initiated trials to total trials and correct responses to initiated trials are > 50%.
Stage 4	5-CSRTT/no-delay	The initiation light is on for 20 sec. If the fish swims to the initiation area, an initiated trial is recorded and one of five choice lights is illuminated for 20 sec. If the fish swims to the illuminated choice area, a correct response is recorded and the feeder releases food with the food light on for 20 sec. This is followed by 10 sec ITI. The 5-CSRTT/no-delay stage is repeated for 30 trials. Fish move

		to the next stage when the average of both initiated trials to total trials and correct responses to initiated trials are > 50%.
Stage 5	5-CSRTT/variable-delay	The initiation light is on for 20 sec. If the fish swims to the initiation area, an initiated trial is recorded and after a variable pre-stimulus interval of 0-8 sec, one of five choice lights is illuminated for 20 sec. This is followed by 10 sec ITI. If during the pre-stimulus interval, the fish swims to any unilluminated choice area, a premature response is recorded. The average of premature responses to initiated trials over four days is reported as a measure of impulsive action.

1241